CHALMERS

Designing Feeding Network for Multi-band MIMO Antenna

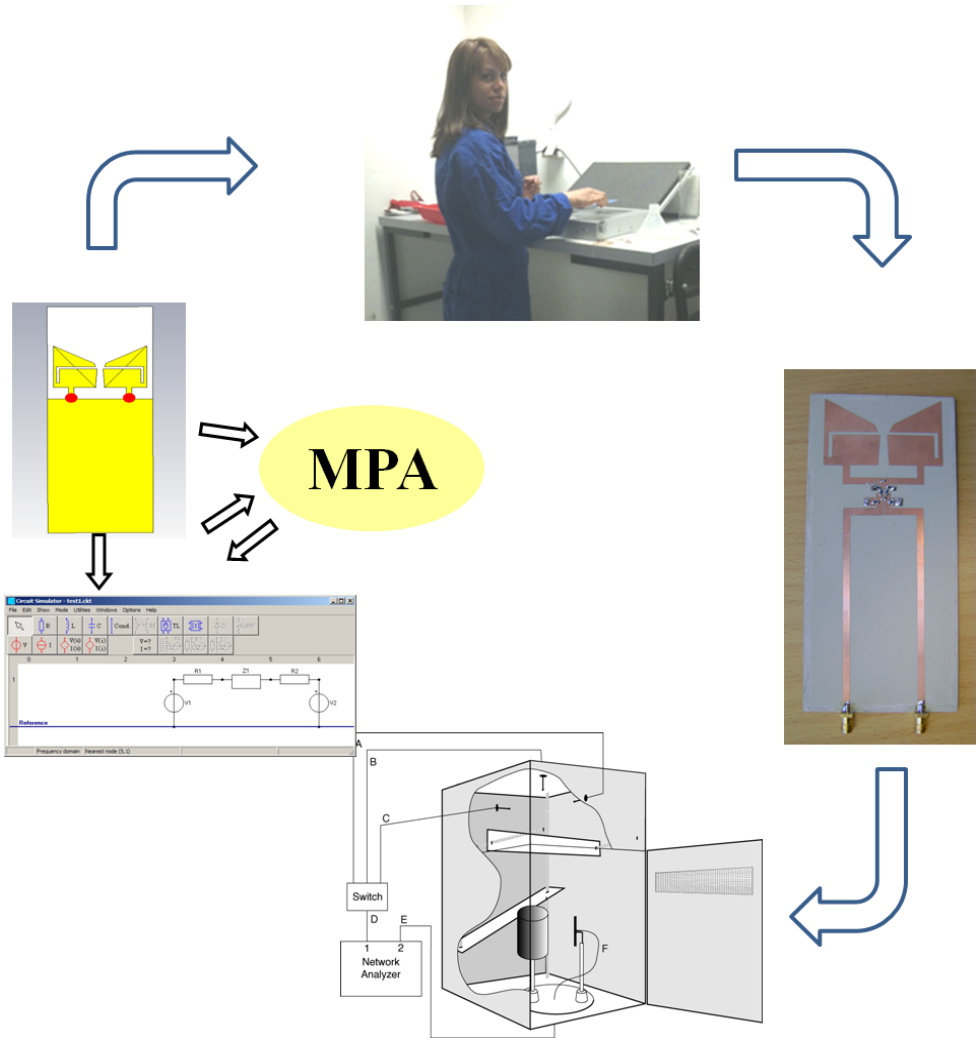

Master of Science Thesis in Wireless and Photonics Program

Mona Hashemi

Designing feeding network for multi-band MIMO antenna

Mona Hashemi

Examiner: Prof. Per-Simon Kildal

Antenna Group, Department of Signals and Systems
Chalmers University of Technology
SE-412 96 Gothenburg
Sweden, 2010

Abstract

This report deals with numerical design of two different feeding networks for multi-band operation of a two-port MIMO antenna at 800/900/1800/2100/2700 MHz for mobile communication applications. It mainly focus on finding a suitable topology for the passive network as to cover the frequency bands of interest. It was found that it was not possible to find a single network covering the whole frequency band, so instead two different networks were designed. One network is designed to improve antenna performance in the lower frequency band 800 to 900 MHz and the other to improve the radiation performance at 1800/2100/2700 MHz. The original two-port antenna proposed by Sony Ericsson was designed for the frequency range x – y GHz so it was scaled and modified for operation in the frequency range 700 MHz to 3 GHz. The modified antenna was manufactured and measurements were done on it, both without and with the designed low-frequency feeding network. The measurement results show that the effective diversity gain was improved by approx. 2 dB in the frequency range 700 – 857 MHz with the feeding network. At frequency of 800MHz, effective diversity gain improves by 2.5 dB to 8 dB. This agrees quite well with what was expected from simulations.

Key words: Multi-port antenna, diversity gain, embedded element efficiency , total radiation efficiency, correlation

Acknowledgment

First I would like to express my gratitude to Professor Per-Simon Kildal and Thomas Bolin for giving me the chance to work on this project. I would also like to thank my supervisor Professor Jan Carlsson for his invaluable and expert scientific guidance during my thesis. I would like to extend my appreciation for his patience guidance in various problems in my thesis. A special thanks to Dr. Kristian Karlsson, my co-supervisor at SP, who introduced me to the simulation tools early on and supported me with excellent comments during the thesis. I would also like to express my gratitude to Thomas Bolin and Zhinong Ying my co-supervisors at Sony Ericsson who have supported me when I had questions during the thesis and with the components and materials needed for realizing the hardware. Finally I would like to thank all the members of the antenna group at Chalmers for always being supportive and helpful. This thesis would simply not exist without the help from all of you.

Preface

This report is the master thesis for the Wireless and Photonics program at Chalmers University of Technology in Gothenburg, Sweden. It was conducted at the Antenna group in the Department of Signals and Systems under the supervision of Professor Jan Carlsson and Dr. Kristian Karlsson. The work was done from mid January through August in the year 2010.

Sony Ericsson in Lund is sponsoring financially this study for one student. Co-supervisors at Sony Ericsson have been Thomas Bolin and Zhinong Ying.

The examiner for this master thesis project is professor Per-Simon Kildal. The project has been done within the framework of the VINN Excellence Center Chase at Chalmers and represents a part of the in-kind of Sony Ericsson Mobile Communications in Lund.

The task has been to analyze and improve the performance of a diversity antenna by introducing different passive network topologies connected to the two ports of a MIMO antenna given by Sony Ericsson. This work suggests two different networks for covering the whole frequency band of interest 800/900/1800/2100/2700 MHz.

Simulations in this work have been done by the commercial EM solver CST MS [1] and the MPA (Multi-Port Antenna evaluator) software [2] developed in the MIMO Terminals project in Chase.

Table of Contents

1 Background

New generations of mobile communication require terminals functioning in multi frequency bands with several antennas. This requirement creates challenges in design of the handsets. Physical size of mobile handsets imposes some challenges as well. Therefore, introduction of new techniques is needed to reduce the constraints for the antenna designer. By utilizing multiple input/output (MIMO) antenna(s) for the radio receiver and transmitter, spatial or polarization diversity can be achieved without additional bandwidth or transmit power. However, it is still challenging to obtain un-correlation or good-enough isolation between the antenna elements, specially at low frequency bands (700-900 MHz) without increasing the physical size of antennas.

One solution to design multi-port antennas in limited space is a method that uses an appropriate matching network connected to the ports in order to achieve improvement in the performance of the antennas. By introduction of passive circuit elements or parasitic structures adjacent to the antennas, decrease in the correlation and higher isolation between antenna elements and thereby increase in the radiation efficiency can be achieved.

Within the CHASE research program, a simulation tool for multi-port antenna analysis and optimization (MPA) has been developed. This makes it possible for the antenna designer to compute all relevant antenna parameters such as diversity gain, radiation efficiency, etc. and furthermore by means of optimization of circuit component in the network connected to the antenna ports improve the performance. The improvement can be in terms of circuit as well as radiation characteristics such as e.g. efficiency and diversity gain which is accomplished by reducing the coupling and correlation between the antenna elements.

1.1 Goal of Project

The extent of this master's thesis work is to analyze and improve -by means of software, commercial as well as developed in Chase, the performance of a given antenna designed by Sony Ericsson. A discrete set of frequencies (800/900/1800/2100/2700 MHz) should be considered and the improvement achieved by connecting discrete circuit elements to the antenna ports. The final goal is to eventually end up with a functioning antenna that performs according to a given specification.
The road leading there can be divided into five parts:

1. Modification of the antenna: The proposed antenna by Sony Ericsson was not designed to work in the frequency range of interest. Thereby, scaling and modification of the original antenna is needed as a first step. Also some optimization in CST is needed to be done to change the shape of the antenna slots to improve its performance at lower frequency bands.

2. Finding matching network: By adding appropriate passive elements to the feeding network of the two-port antenna, it is possible to achieve better performance at frequency range of interest. Hence, an intelligent guess based on circuit theory is needed to start with and find a network topology that can satisfy the specifications. A circuit simulator program and MPA (multi-port antenna evaluator) software should be used as simulation tools to design the circuit and compute and analyze the radiation parameters of the antenna connected to the network.

3. Optimization: With the help of MPA and circuit simulator, optimizations are done focusing on circuit components connected to the two-port antenna to improve radiation characteristics such as diversity gain and total radiation efficiency.

4. Realization: Applying everything that is needed to build the prototype, the designed antenna itself and also the designed antenna with the matching network connected to it which needs some precise soldering techniques and also photo lithography and etching for realizing the antenna.

5. Measurement: The last step is to measure the fabricated antennas in the reverberation chamber at Chalmers and compare the measured diversity gain and radiation efficiency with simulated values.

1.2 Studied Antenna Parameters

In order to characterize multi-port antennas to be used in multipath environment we use the so called embedded element approach. In this context an embedded element is defined as an antenna element in the multi-port antenna when all other elements are terminated. The termination impedance can, in principle, be anything from short to open circuit, but normally 50 ohm is used as termination on all ports [3],[4],[5].

The far-field functions/radiation patterns of the embedded elements play an important role in describing MIMO/diversity antennas. The embedded element pattern represents the radiation from the multi-port antenna when one of the antenna elements is excited and all other ports are terminated. In a multipath environment, each antenna element transmit or receive the signals incoherently relative to the other elements, therefore each element transmit or receive signals through its embedded far field function. From the corresponding far-field, radiation efficiency of each antenna element and correlation between the signals at all ports can be determined [3].

In order to quantify the performance of multi-port antennas, radiation efficiency, correlation and diversity gain are needed. How to determine these parameters will be explained in the next parts.

1.2.1 Total Radiated Power

Total radiated power (P_{rad}) from an antenna can be computed as a surface integral of the far-field radiation patterns:

$$P_{rad} = \frac{1}{2\eta} \iint_{4\pi} \left[\left| E_\theta(\theta,\varphi) \right|^2 + \left| E_\varphi(\theta,\varphi) \right|^2 \right] \sin(\theta) \, d\theta \, d\varphi \tag{1.1}$$

where $E_\theta(\theta,\varphi)$ is the theta component of the electric far field function and $E_\varphi(\theta,\varphi)$ is the phi component and η is the free space wave impedance [4].

1.2.2 Correlation

For MIMO and diversity antennas, the correlation coefficient is of significance in such a way that low correlation is needed for high diversity gain and capacity. Correlation can be computed from the far field embedded patterns as shown below:

$$\rho_{ij} = \frac{\iint_{4\pi} E_i^H E_j \, d\Omega}{\sqrt{\iint_{4\pi} E_i^H E_i \, d\Omega \iint_{4\pi} E_j^H E_j \, d\Omega}} \tag{1.2}$$

where E_i is the electric field when the i:th antenna element is excited, ρ_{ij} is the complex correlation and H is Hermitian transpose. The square of complex correlation coefficient is called envelope correlation coefficient or power correlation [3],[4].

It is also possible to express the complex correlation coefficient in terms of the scattering parameters as described in (1.3) [3].

$$\rho_{ij} = \frac{S_{Iii}^* S_{ij} + S_{ji}^* S_{jj}}{\sqrt{(1 - |S_{ii}|^2 - |S_{ji}|^2)(1 - |S_{jj}|^2 - |S_{ij}|^2)}} \tag{1.3}$$

This formula is limited to passive and lossless antenna elements.

1.2.3 Embedded Radiation Efficiency

In this chapter it will be explained how to calculate the radiation efficiency for embedded elements of a multi-port antenna. Figure 1.1 illustrates a diversity or MIMO antenna consisting of N ports.

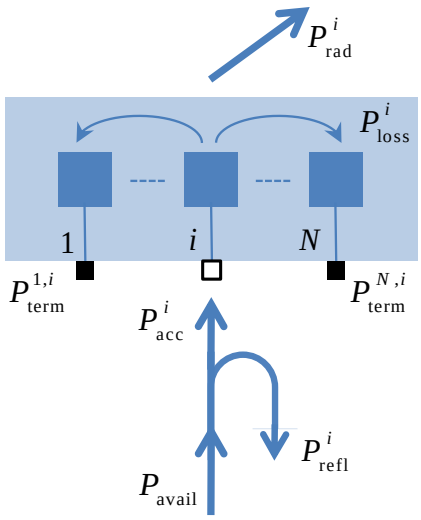

Figure 1.1 Multi-port antenna.

For multi-port antenna, efficiency per antenna element is of interest which is defined as embedded element efficiency. It is calculated for element *i* when the antenna is excited at port i and all other ports are terminated in known impedances (i.e. usually in 50 ohm). There are two types of radiation efficiency. Embedded element radiation efficiency ($e_{\text{emb}}^{i,\text{N-port}}$) which is defined as the ratio of the radiated power to the power delivered to the antenna and total radiation efficiency (e_{totemb}^{i}) which is defined as the ratio of the radiated power to the maximum available power from the generator and can be expressed as: [3],[4],[7],[8]

$e_{\text{emb}}^{i,\text{N-port}} =$ N-port embedded element efficiency for antenna element i

$$e_{\text{emb}}^{i,\text{N-port}} = \frac{P_{\text{rad}}^{i}}{P_{\text{acc}}^{i}} = \frac{P_{\text{rad}}^{i}}{P_{\text{avail}}\left(1-\sum_{j=1}^{N}\left|S_{ji}\right|^{2}\right)} \tag{1.4}$$

$e_{\text{totemb}}^{i} =$ Total embedded element efficiency for antenna element i

$$e_{\text{totemb}}^{i} = \frac{P_{\text{rad}}^{i}}{P_{\text{avail}}} = e_{\text{emb}}^{i,\text{N-port}} e_{\text{decoupl}}^{i} \tag{1.5}$$

$$e_{\text{decoupl}}^{i} = 1 - \sum_{j=1}^{N}\left|S_{ji}\right|^{2} = \text{Decoupling efficiency for antenna element } i \tag{1.6}$$

As can be seen in equation (1.5), the mutual coupling between elements play a significant role in total radiation efficiency. In another words, low coupling is needed for high total embedded efficiency [7],[8].

In the equations (1.4)-(1.5), P_{avail} is the power available from a matched source, P_{acc}^{i} is the power accepted by antenna when excited at port i and P_{rad}^{i} is the radiated power when antenna is excited at port *i* and can be defined as:

$$P_{\text{acc}}^{i} = P_{\text{avail}} - P_{\text{decoupl}}^{i} = P_{\text{avail}}\left(1 - \sum_{j=1}^{N}\left|S_{ji}\right|^{2}\right) \tag{1.7}$$

$$P_{\text{rad}}^{i} = P_{\text{avail}} - P_{\text{decoupl}}^{i} - P_{\text{loss}}^{i} = P_{\text{avail}}\left(1 - \sum_{j=1}^{N}\left|S_{ji}\right|^{2}\right) - P_{\text{loss}}^{i} \tag{1.8}$$

where

$P_{\text{decoupl}}^{i} =$ Power dissipated in all terminations for excitation at port i

$$P_{\text{decoupl}}^{i} = P_{\text{avail}} \sum_{j=1}^{N}\left|S_{ji}\right|^{2} \tag{1.9}$$

And $P_{\text{term}}^{j,i} =$ Power dissipated in matched load at port j due to excitation at port i

$$P_{\text{term}}^{j,i} = P_{\text{avail}}\left|S_{ji}\right|^{2} P_{\text{term}}^{j,i} \tag{1.10}$$

1.2.4 Diversity Gain

Diversity antenna uses two or more branches of antennas to improve the quality and reliability of wireless link. There are several types of diversity, spatial, pattern and polarization diversity. By using this technique, the received signals will be uncorrelated on ports in a receiver system. In a two-port antenna for instance, by selecting an appropriate combination of the two signals, the probability of low fading dips in the combined signal will be strongly decreased. Several different combination schemes such as selection combining, switch diversity and maximum ratio combining can be used.

With selection combining 10.2 dB improvement can be achieved in cumulative distribution function (CDF) of the combined signal relative to the cumulative distribution function (CDF) of received signal at one of the two antenna ports of the diversity antenna at 1% CDF level [3],[9].

As can be seen in Figure 1.2, depending on what kind of reference is used in comparison between CDF levels, different diversity gains can be introduced.

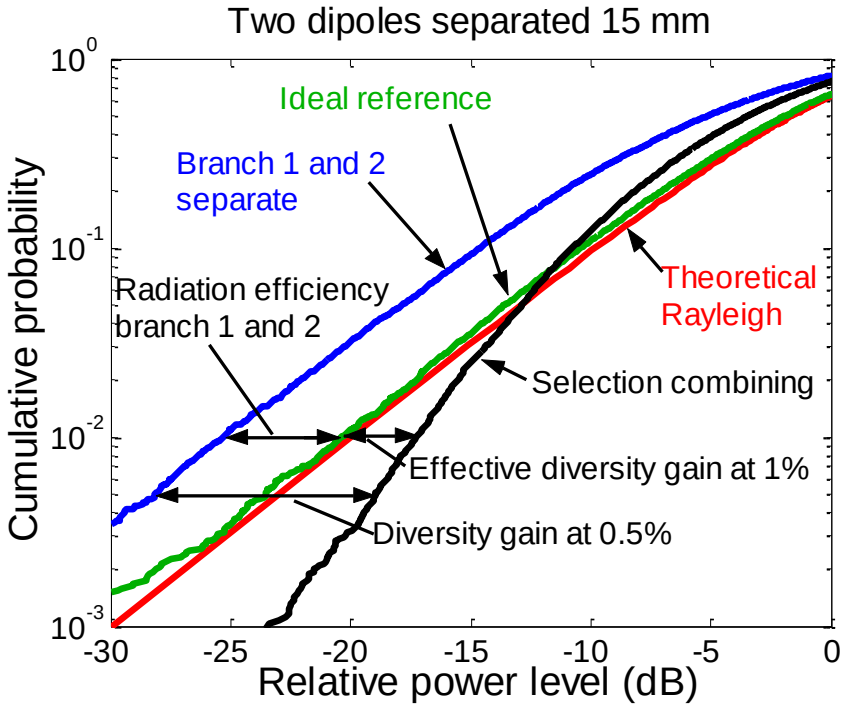

Figure 1.2 *Cumulative probability distribution function (CDF) of measured transmission function in reverberation chamber for ideal reference antenna and diversity antenna consisting of two parallel dipoles [3].*

Apparent diversity gain (ADG) is defined as the difference between cumulative probability distribution function (CDF) of diversity-combined signal and the CDF of the signal received by the element from the antenna with the better average signal level at 1% CDF level [3],[9]. Instead of reading the ADG from the CDF-curves it can be obtained from the correlation coefficient. It is shown in [10] that calculating the ADG from eq. 1.11 is much more accurate. For a two-port antenna, and using selection combining scheme, the ADG can be computed as:

$$ADG = 10.48\sqrt{1 - 0.99\left|\rho^2\right|} \tag{1.11}$$

ADG for an N-port antenna using selection combining can be expressed as:

$$ADG = D_{Nbranches}\sqrt{1 - 0.99\left|\max(\rho_{ij})\right|^2} \tag{1.12}$$

In case the antenna elements have different embedded radiation efficiencies, diversity gain of a two-port antenna can be obtained as [11].

$$ADG^{SC} = \sqrt{1 + (ADG_{\max}^{SC\ 2} - 1)\frac{e_{\min}}{e_{\max}}(1 - \rho^2)} \tag{1.13}$$

where $ADG_{\max}^{SC}$ for two-port antenna is 10.48 (i.e. 10.2dB).

Effective diversity gain (EDG) is defined as the difference between cumulative probability distribution function (CDF) of diversity-combined signal and the CDF of the signal at the port of an ideal single antenna (corresponding to radiation efficiency of 100%, i.e. 0 dB) at 1% CDF level. It can be expressed as:

$$EDG = e_{totemb} \; ADG \tag{1.14}$$

Actual diversity gain is defined as the difference between CDF of the signal at the port of an existing practical single antenna that is to be replaced by the diversity antenna at 1% CDF level.

1.2.5 MIMO Capacity

MIMO systems uses multiple transmit antennas on the transmit side and multiple receiver antennas on the receive side to improve communication performance. Many bits can be transmitted per second for a specific bandwidth and the data is distributed among the transmit channels and combined after reception in such a way that the overall channel capacity is maximized [3],[4].

A MIMO system consisting of M_t number of transmit antenna elements and M_r number of receive antenna elements can be describes as:

$$y = Hx + w \tag{1.15}$$

Where y is the received signal, x is the transmitted signal, w is additive white noise and H is the channel matrix of size $M_r \times M_t$.

Capacity in MIMO systems can be divided in two major groups: capacity and outage capacity where outage capacity is the capacity that is guaranteed with a certain level of reliability. MIMO system capacity is the capacity over a $M_r \times M_t$ communication channels in a certain environment and the upper limit of MIMO system capacity is the ergodic capacity. When the channel in unknown to the transmitter, uncorrelated signals of equal power are transmitted on each antenna. The MIMO system capacity during maximum ratio combining can be expressed as Shannon's capacity formula [3],[4].:

$$C = \log_2 \left(\left| I_{M_r \times `M_r} + \frac{SNR}{M_t} H_{M_r \times `M_t} H^*_{M_r \times `M_t} \right| \right) \tag{1.16}$$

where

C is the capacity in bits/s/Hz

M_t is the number of transmit antennas

M_r is the number of receive antennas

$I_{M_r \times `M_r}$ is the identity matrix with dimension M_r by M_r

$H_{M_r \times `M_t}$ is the normalized complex channel matrix

$H^*_{M_r \times `M_t}$ is the complex conjugate transpose of the channel matrix

Figure 1.3 is an example to show how an average Shannon capacity varies as a function of SNR for four different cases, named as SISO, SIMO with MRC at the receiver end , 2x2 MIMO with un-informed transmitter and 2x2 MIMO with water filling at the transmitter. The frequency is 1800 MHz and the antenna separation is 0.15 wavelengths [12].

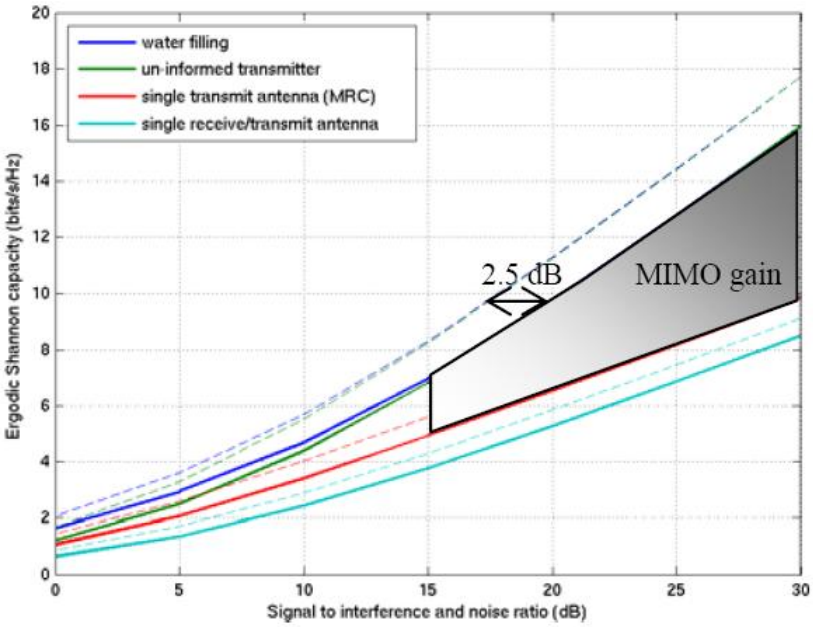

Figure 1.3 Average Shannon capacity of two closely spaced (0.15 wavelengths) parallel dipoles (solid lines) and two crossed dipoles (dashed lines) in a uniform 3D environment as a function of SNR, from [12].

2 Numerical Simulations

In this work, the antenna is designed in the full-wave electromagnetic simulator CST microwave studio. Port response matrix –scattering matrix in this work- and embedded element patterns –radiation from the multi-port antenna when one of the ports is excited and the other is terminated- are computed by CST simulator. These data are imported to a software called MPA (Multi-Port Antenna evaluator). MPA is used for computing and optimizing all relevant antenna parameters such as radiation efficiency, diversity gain, correlation, etc. It is also connected actively with a circuit simulator and can optimize the matching network for the given two-port antenna [11].

2.1 Full Wave Simulator (CST)

A full-wave electromagnetic field simulator such as CST models and computes the interaction of electromagnetic fields with the physical object and environment. The software efficiently uses Maxwell's equations to calculate antenna performance, electromagnetic compatibility, radar cross section and electromagnetic wave propagation, etc. [1].

2.2 Combination of Full Wave and Circuit Simulator

The method is using a full-wave electromagnetic field simulator such as CST design studio in combination with a standard circuit simulator. The advantage is that when optimizing for a multi-port antenna by MPA software, only a few full-wave simulations -which are usually time consuming- are needed. By this means calculations of radiation properties of multi-port antennas will be more efficient and less time consuming [2],[11]. Figure 2.1 shows the combination of full-wave simulator, circuit simulator together with MPA software.

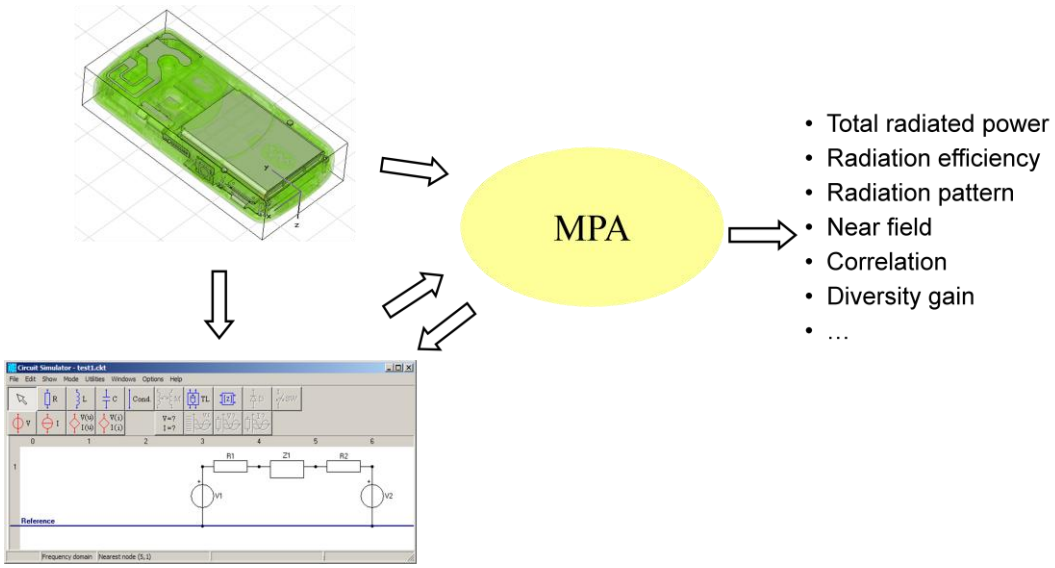

Figure 2.1 Combination of Full-wave simulator, circuit simulator together with MPA software.

Methodology is that a set of embedded element patterns and a port response matrix such as scattering matrix are computed by a full-wave simulator program e.g. CST. The embedded element patterns represent the far-field radiation from each single element of an N-port

antenna when one of the port is excited and all the others are terminated. That means for an N-port antenna, N embedded element pattern need to be computed. The computed port response matrix is exported to a circuit simulator program in presence of any feeding network and then the currents at the antenna ports can be computed. Afterwards, computed new port currents is weighted by the previous embedded element patterns in order to compute the total radiation from the multi-port antenna with the network [4], [11].

To clarify the method more, here comes a simple example. Consider a two-port antenna, the procedures is as follow [11]:

1. Compute current feeding port1 (I_{11}) and current induced in port2 (I_{21}) and embedded element pattern(E_1), when antenna element1 is excited and element2 is terminated.

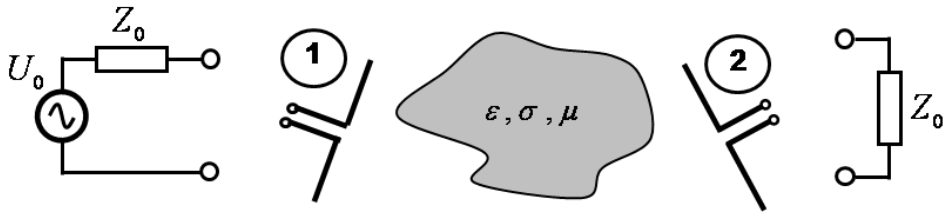

Figure 2.2 Two-port antenna, port1 is excited and port2 is terminated [11].

2. Repeat step1 for antenna element2. Compute (I_{22}),(I_{12}),(E_2).

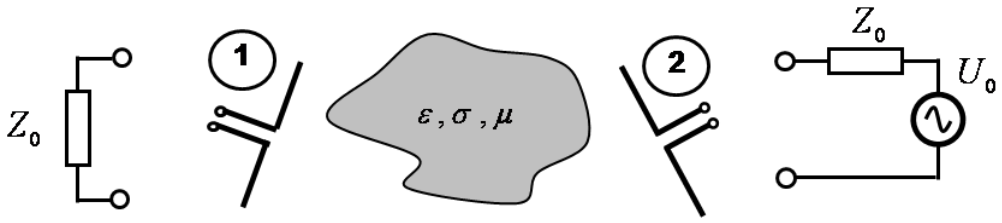

Figure 2.3 Two-port antenna, port2 is excited and port1 is terminated [11].

3. Form the port response matrix from steps1 and 2.

$$\begin{bmatrix} I_{11} & I_{12} \\ I_{21} & I_{22} \end{bmatrix}$$

At this point, by using only a circuit simulator, the total radiation can be computed for general case as is depicted in Figure 2.4 Two-port antenna, general case [11].

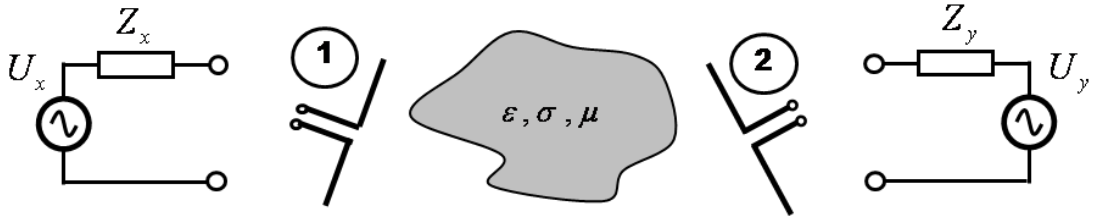

Figure 2.4 Two-port antenna, general case [11].

4. Use a circuit simulator program and import the port response matrix and connect networks to the ports and calculate currents to the ports (I_x), (I_y).

$$I_x = \alpha I_{11} + \beta I_{12}$$
$$I_y = \alpha I_{21} + \beta I_{22}$$

5. Calculate the radiation pattern for the two-port antenna in presence of connected network :

$$E = \alpha E_1 + \beta E_2$$

where

$$\begin{bmatrix} \alpha \\ \beta \end{bmatrix} = \begin{bmatrix} I_{11} & I_{12} \\ I_{21} & I_{22} \end{bmatrix}^{-1} \begin{bmatrix} I_x \\ I_y \end{bmatrix}$$

It should be added that radiation pattern obtained from step 5 can be processed to give radiation parameters such as: diversity gain, correlation, radiation efficiency, etc.

MPA is a computer code that is based on the theory explained above. It imports the data from a commercially existing full-wave simulator for computing the port response. Output of MPA is in principle radiation parameters such as radiation efficiency, correlation, etc. [11].

3 The Antenna

In this chapter, procedure related to the antenna design in CST is explained. Original antenna [14] is used as a starting point and modifications and down scaling have been done for better performance at lower frequency bands (800-900 MHz). Afterwards the simulated antenna has been manufactured and measurements have been done to validate the simulations.

3.1 The Original Design

A compact ultra wideband MIMO/diversity antenna has been designed to work in 3.1-10.6 GHz spectrum for UWB applications [14]. MIMO and diversity systems require an increase of isolation between antenna elements. Through a tree-like structure introduced in [14], an isolation better than -16 dB and impedance bandwidth (S11<-10 dB) covering the UWB band of 3.1-10.6 GHz has been achieved. The antenna is shown in Figure 3.1 where the antenna elements as well as the tree-like structure on the back side can be seen. Size of the antenna is 35 x 40 mm.

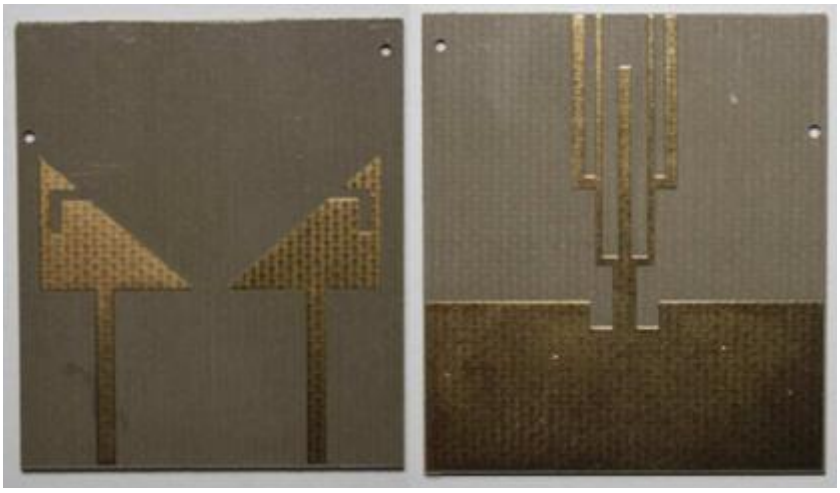

Figure 3.1 Prototype of the proposed UWB MIMO/diversity antenna: (left) top view, (right) back view[14].

The antenna is printed on a dielectric substrate with a relative permittivity of 3.5 and loss tangent of 0.0018. The PCB thickness is 0.8 mm. Each radiator is fed with a 50 ohm microstrip line.

Figure 3.2 shows the proposed antenna and marks the different branches in tree-like structure.

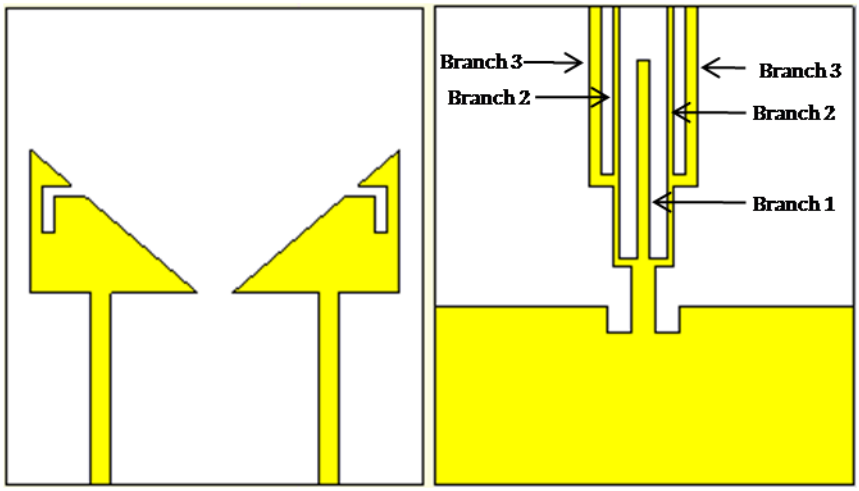

Figure 3.2 UWB antenna with treelike structure on the ground plane,

Figure 3.3 and Figure 3.4 shows the scattering parameters calculated by CST when the total number of tree-branches (see Figure 3.2) varies [14].

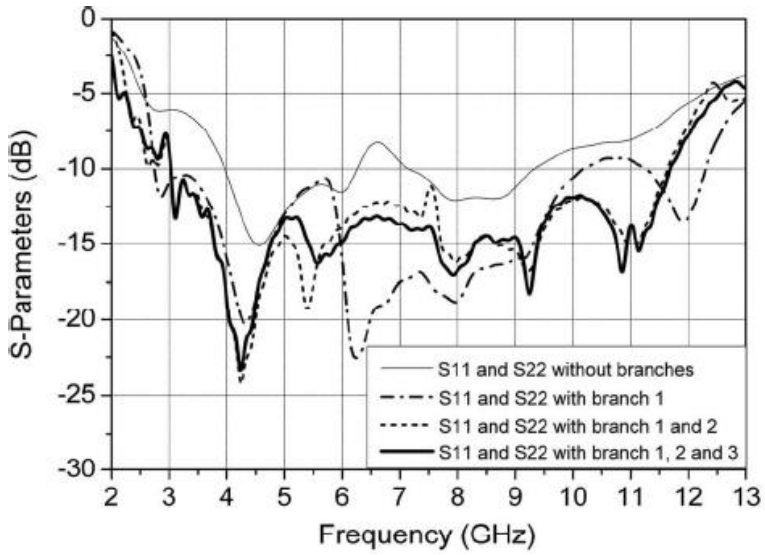

Figure 3.3 Simulated S11and S22 when the total number of branches varies [14].

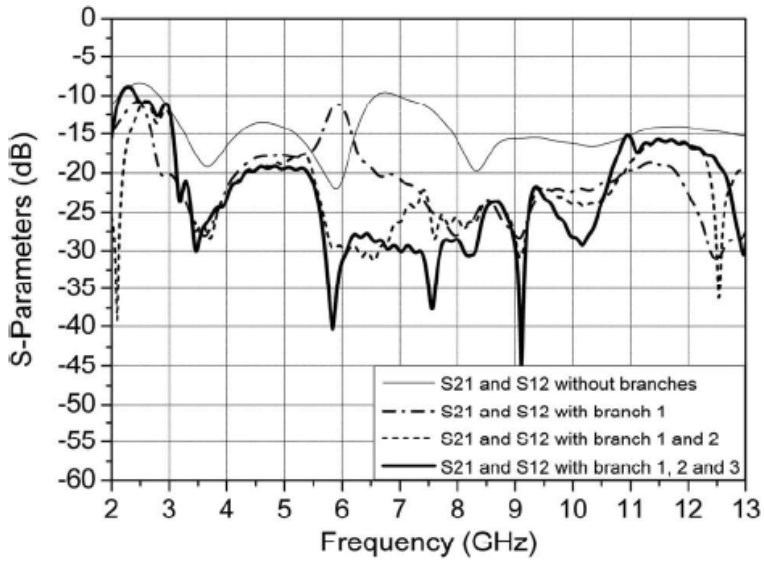

Figure 3.4 Simulated S12and S21 when the total number of branches varies [14].

As it can be seen in the figures wide-band isolation and matching is obtained for the UWB antenna by including the tree-like structure on the ground plane. The reason is that branch1 [see Figure 3.2] acts as a reflector (see [15] and [15]), which can reduce the mutual coupling by separating the radiation patterns of the two radiators. Another reason is that as the number of branches of the tree increases, more resonances occurs, each of which is provided by a monopole of one branch or a quarter-wavelength slot formed by two neighboring branches [14]. On the other hand, having the tree-like structure in the antenna design occupies space by adding to the antenna length which is sometimes a drawback. One possible way to obtain the wanted isolation but in smaller space could be to introduce a feeding network between the antenna elements. However achieving wide-band performance is challenging and have not been realized yet, but this is a study work in this thesis to be figured out in the next chapters.

3.2 The Modified Design

Figure 3.5 shows the modified antenna modeled in CST. As can be seen in this figure, the proposed antenna has been scaled and modified when compared to the original antenna shown in Figure 3.1. Radiators are scaled by a factor of two and re-shaped for low frequency improvement. Antenna size is 162 x 62 mm and it is printed on a dielectric substrate Arlon 25FR with a permittivity of 3.58, thickness of 1.473 mm and loss tangent of 0.003. Radiators are made of copper with a thickness of 45 μm. The antenna ports are fed with 50 ohm microstip lines of 3.4 mm width.

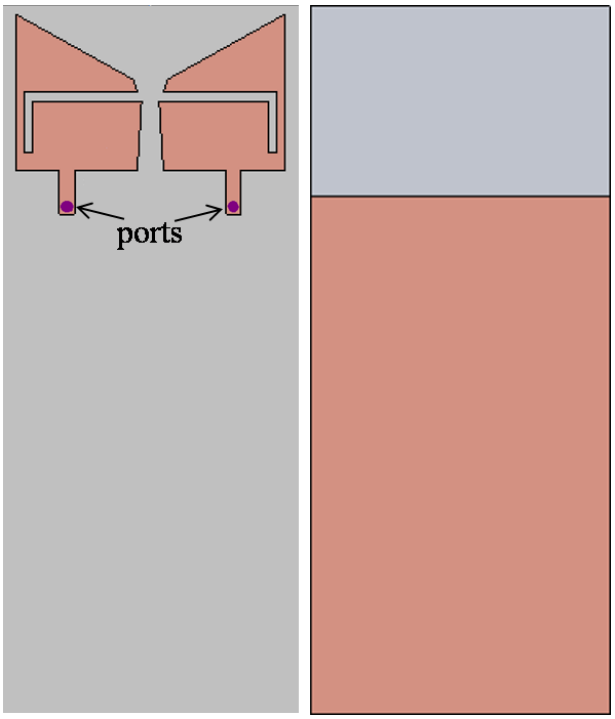

Figure 3.5 Modified and scaled antenna in CST MS, antenna dimension is 162 x 62 mm.

Simulated scattering parameters are shown in Figure 3.6 and Figure 3.7. As can be seen in equation (1.6), in order to have high total radiation efficiency, both mutual coupling between antenna element 1 and 2 and also reflection coefficient S11 and S22 should be low enough. The goal is to have S11 less than -6dB and S21 less than -10dB.

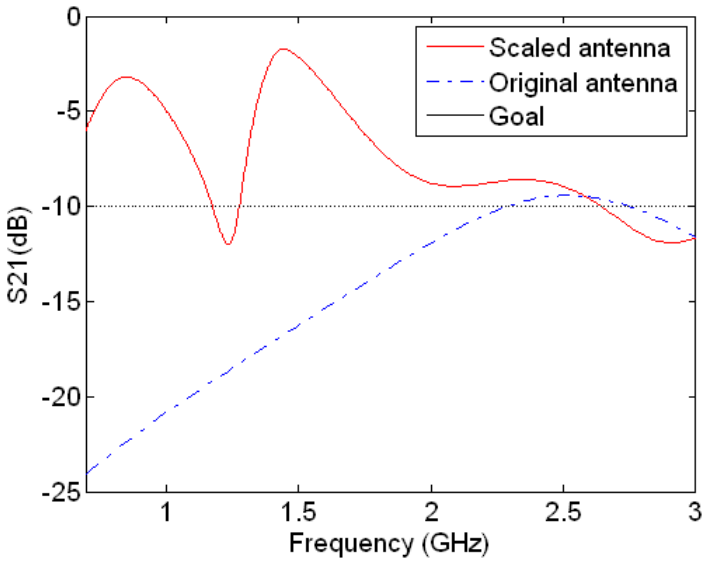

Figure 3.6 Simulated S21 for original antenna and modified antenna from 0.7 to 3 GHz.

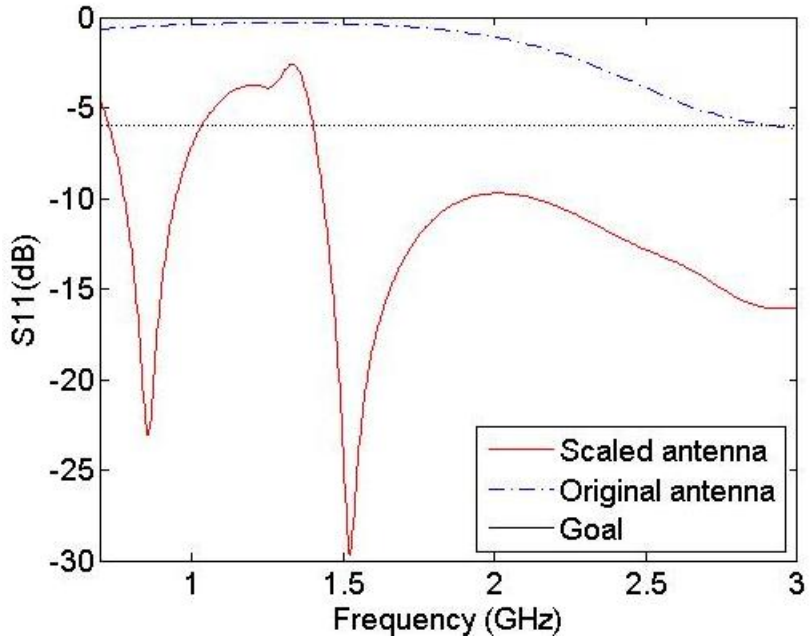

Figure 3.7 Simulated S11 for original antenna and modified antenna from 0.7 to 3 GHz.

As can be seen in the Figure 3.7, the original antenna does not radiate at low frequencies and almost all the power fed to the antenna ports are reflected. In the modified scaled antenna, matching at low frequencies is improved but mutual coupling between the antenna elements are high in frequencies of interest 800/900/1800/2100/2700.

3.3 Fabricated Antenna

First step before designing the feeding network is to build the scaled antenna and perform measurement to check the agreement between simulations and measurement. This measurement is a baseline for checking the accuracy of the design. It is obvious that the agreement should be better at this stage. Since adding passive lumped elements will add uncertainties in the components, it is probable that the agreements at this stage is expected to be better than what is going to be when connecting feeding network to the antenna. The designed antenna is manufactured by photolithography and etching method at SP. Measurements is done in the Bluetest reverberation chamber at Chalmers antenna lab. In the following chapter simulation results is compared with the measurements.

Figure 3.8 *Prototype of the designed MIMO/diversity antenna: (left) top view, (right) back view.*

Figure 3.9 shows envelope correlation coefficient from the simulation results and measurement. As can be seen, correlation is higher in measurements, thus considering equation (1.11) measured apparent diversity gain is expected to be less than simulation as well. The agreement is good except around 1.45 GHz. However, correlation coefficient is low at frequencies of interest.

Figure 3.9 shows the simulation and measurement data for correlation. The agreement is good except around 1.45 GHz. However, correlation coefficient is low at frequencies of interest.

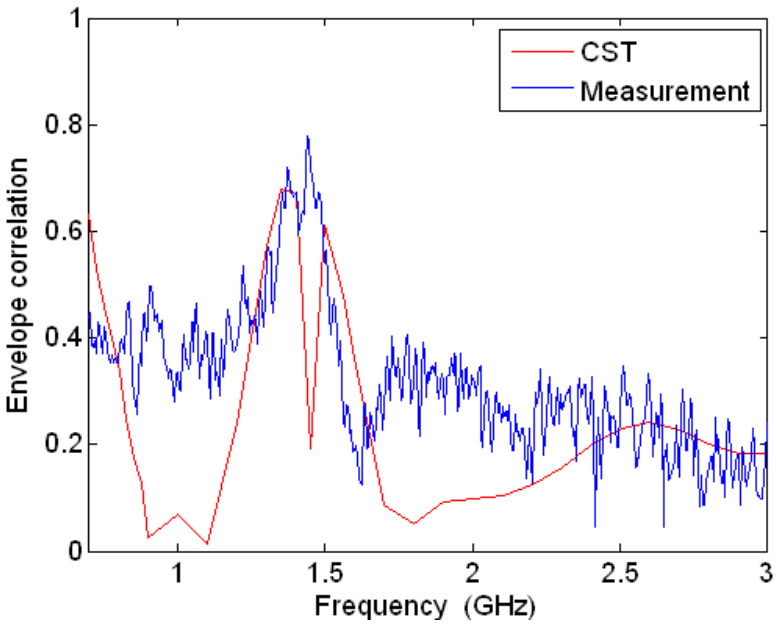

Figure 3.9 *Data for Envelope correlation coefficient, simulation and measurement.*

Figure 3.10 shows the measured data for total radiation efficiency in comparison with simulation results. The difference between measurement and simulations is +/- 0.5 dB except at frequencies below 1GHz which is 1.5 dB at worst. It can be seen that antenna element2 has a better agreement with simulation. The reason can be due to the fact that measured data have statistical variations and also there could be some asymmetric difference in the hardware of antenna. There is a difference in resonance frequency for the two elements. A reason can be that there are some differences in the geometry of the two elements, i.e. they are not exactly equal. This could be due to tolerances in the manufacturing.

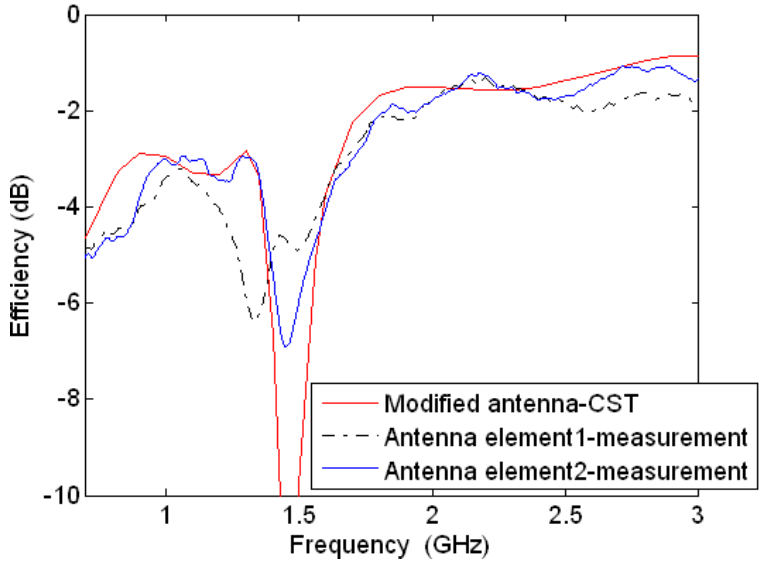

Figure 3.10 Data for total radiation efficiency, simulation and measurement.

Figure 3.11 and Figure 3.12 shows apparent diversity gain and effective diversity gain respectively. The difference between measurement and simulations is less than +/-1 dB and measurement curve follows the simulation data properly. It can be seen that at frequency of 1.45 GHz, simulated diversity gain is higher than measurement that is in agreement with lower correlation in simulation data in Figure 3.9 that was mentioned before.

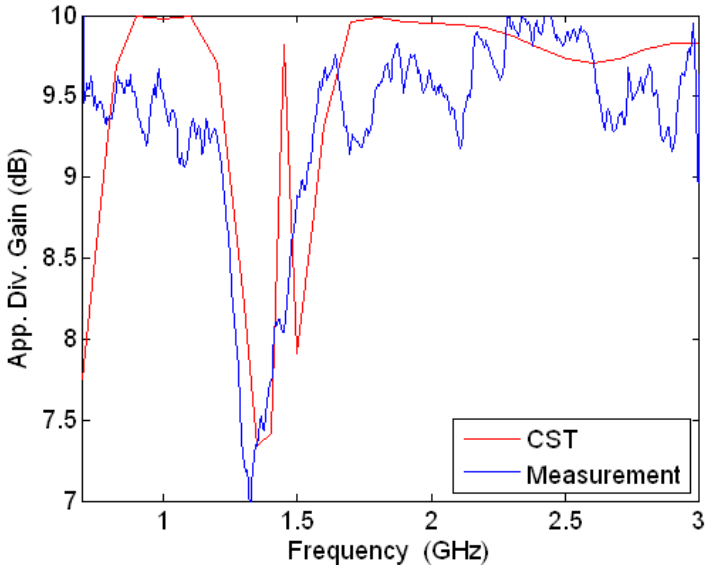

Figure 3.11 Apparent diversity gain, simulation and measurement data.

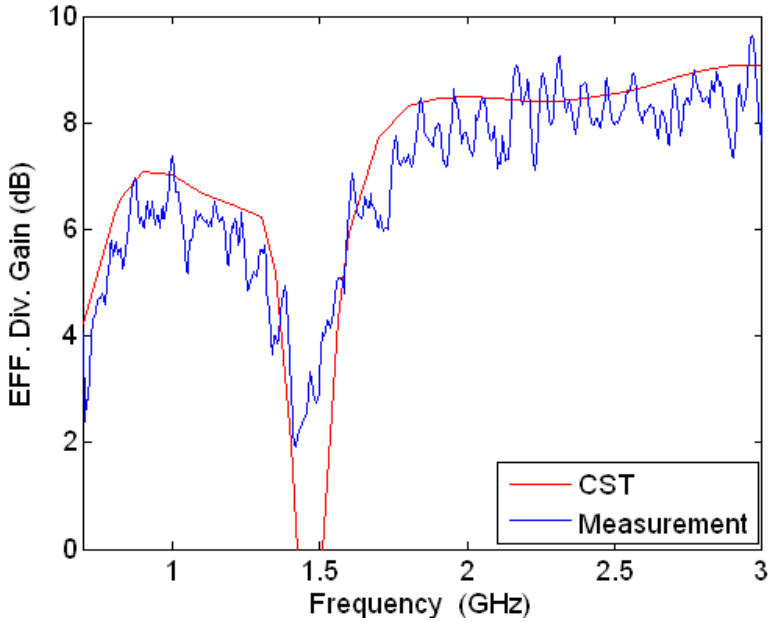

Figure 3.12 Effective diversity gain, simulation and measurement data.

Figure 3.13 and Figure 3.14 shows measured mutual coupling and reflection coefficient in comparison with simulated ones. The difference between simulation and measurement is acceptable; however, the difference increases at higher frequencies of 1.6 to 2.2 GHz.

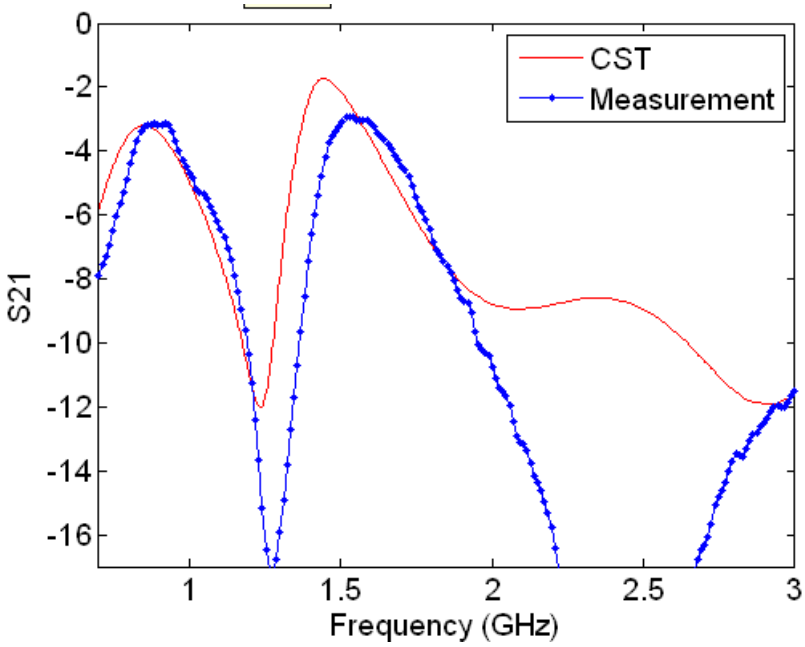

Figure 3.13 Simulated S21 for modified antenna from 0.7 to 3 GHz.

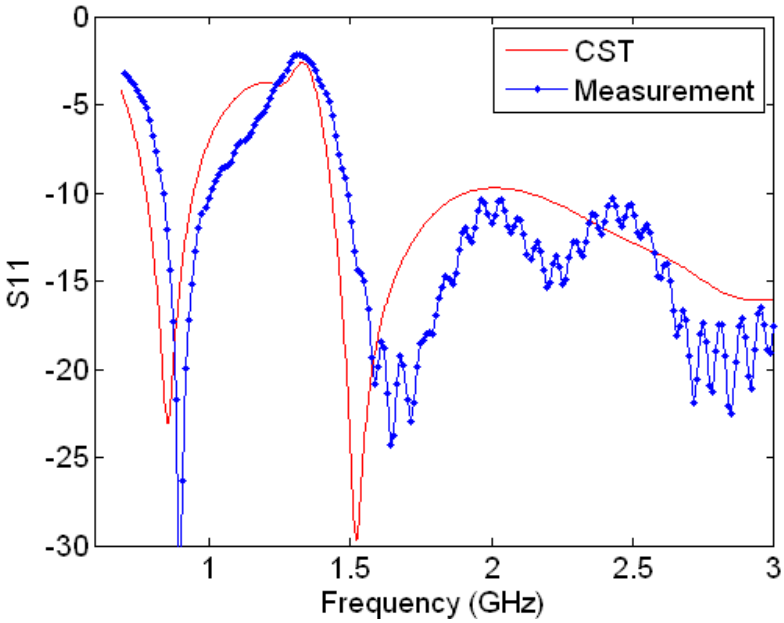

Figure 3.14 Simulated and measured S11 for modified antenna from 0.7 to 3 GHz.

The next logical step is to go further and aim to find and design the matching network with help of MPA software -which is explained in chapter 2- for improvement of antenna performance specially at low frequencies of 800-900 MHz.

4 Matching Network

In this chapter, several networks were tested in order to find the appropriate one for the feeding network of the antenna. I also tried to explain how to find the appropriate topology for the feeding network connected to the antenna ports and challenges regarding finding a solution that can improve antenna performance at a discrete set of frequencies. In 4.2, optimization procedure -which is done by MPA software- is explained and results from the network topologies which gave the best improvement in antenna radiation properties are shown. The aim is to find a network that can produce wideband performance at the frequencies of interest 800/900/1800/2100/2700 MHz.

The main goal is to figure out if the wanted improvement in performance is possible to achieve with a single passive network connected to the antenna ports or not.

4.1 Different Topologies

The goal is to try to find a network that can reduce the mutual coupling between the antenna elements, thus increasing the total embedded radiation efficiency (see equation (1.5)). The matching network should also satisfy wideband matching of antenna ports to the 50 ohm generator impedance. If it is possible to achieve these two aims, radiation parameters such as correlation, total radiation efficiency and hence effective diversity gain will be improved (see equation (1.3), (1.5) and (1.14).

The circuit simulator program CircSim [17] is used to design the feeding network connected to the ports of the antenna[17].

In the figures below, Z1-Z10 are passive components with complex values, thus representing general components. The antenna is defined as a two-port component for which the scattering parameters are imported from simulation done in CST. Port1 and port2 are defined between antenna element1 and antenna element2 and the ground plane, respectively. V1 and V2 represent generators and R1 and R2 are 50 ohm source impedances.

Figure 4.1 is the simplest possible passive network. Several optimizations have been done but it is not possible to achieve good results for either correlation or efficiency. The reason can be due to lack of component between antenna ports. A component between ports can make a possible feedback between antenna elements for decreasing mutual coupling between them.

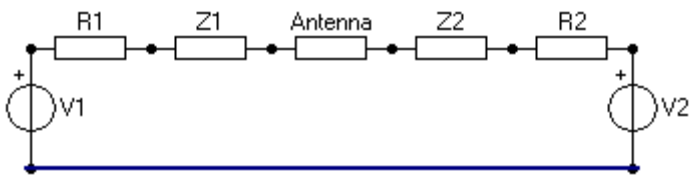

Figure 4.1 Network topology1 connected to the antenna.

In Figure 4.2 and Figure 4.3 are shown the possible passive networks connected to the antenna that can help to improve radiation performance. The reason to choose these topologies is that a path with capacitance or inductor –depending on the mutual coupling between antenna elements- is needed between the ports to reduce the coupling between them.

Z1 and Z2 are placed between source impedances and antenna ports to improve the matching to 50 ohm.

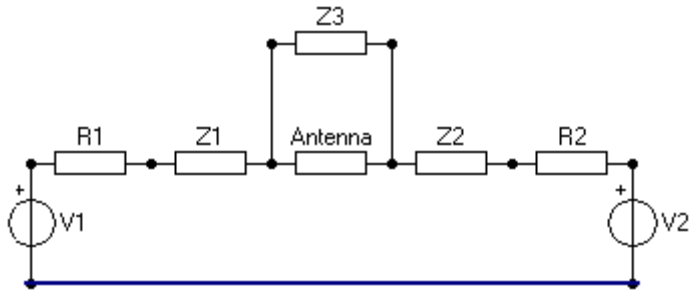

Figure 4.2 Network topology2 connected to the antenna.

Both network2 and network3 can improve efficiency and effective diversity gain for optimization done at each single frequency. Thus it happens that network3 acts better at low frequency. It is possible to have 9.3 dB effective diversity at 800 MHz with network3 where network2 gives 8.2 dB for effective diversity gain. Also at 824 MHz, effective diversity gain drops for antenna with network2 to 6.5 dB where optimization gives 9 dB of effective diversity gain for the antenna with network3.

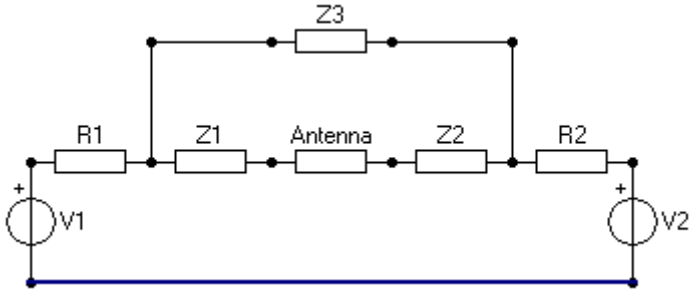

Figure 4.3 Network topology3 connected to the antenna.

As explained before for network1, since there is no path for reducing mutual coupling between antenna elements, no acceptable optimization results were found for effective diversity gain of network4.

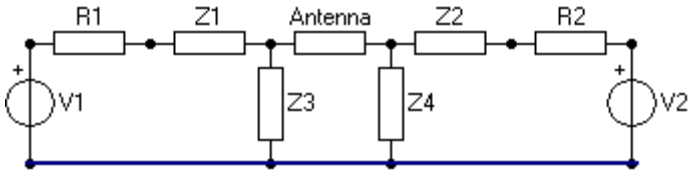

Figure 4.4 Network topology4 connected to the antenna.

Figure 4.5 and Figure 4.6 are more complex topologies with more components. It is maybe possible to obtain a more wideband improvement with these two networks which will be investigated in the next part.

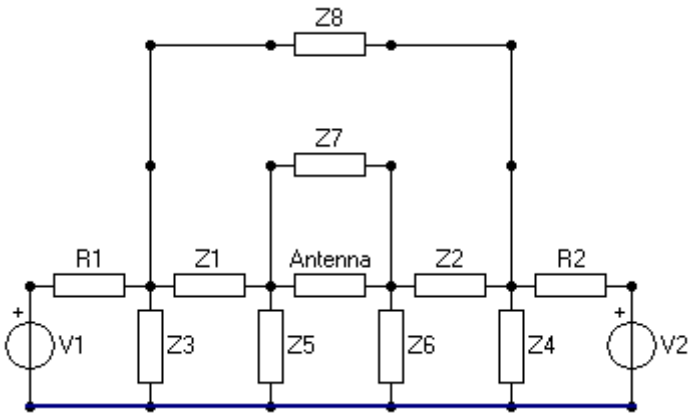

Figure 4.5 Network topology5 connected to the antenna.

The matching network connected to the antenna can be seen as a four-port network. Two ports are connected to the generators and two to the antenna ports. As a result the matching network can be seen as a 4 x 4 matrix. This means that up to 16 passive elements are needed, but due to the symmetry in the antenna, 10 components is enough for realizing the network. Such a network is network6 which is shown in Figure 4.6.

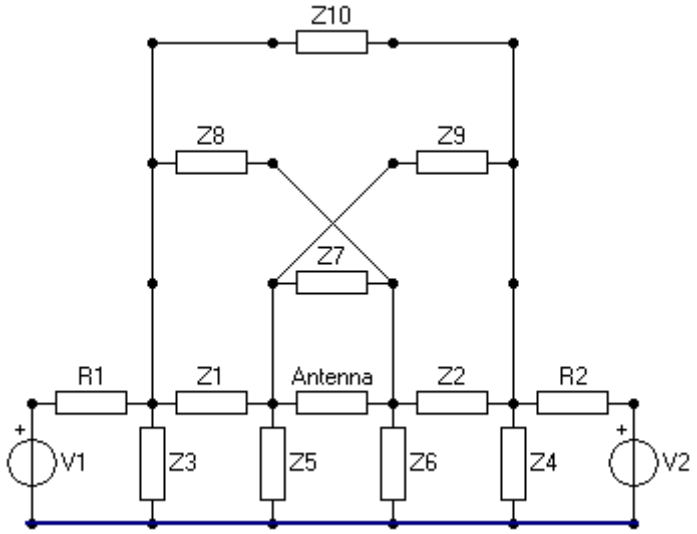

Figure 4.6 Network topology6 connected to the antenna.

4.2 Optimization

There are several steps that is needed to be done before starting the optimization. Steps 1 to 7 explains the optimization procedure.

1) S-matrix and embedded element patterns of the original antenna are computed in CST.

2) The S-matrix is converted to a Z-matrix, this can be done by CircSim.

3) The Z-matrix of original antenna is imported as a component in CircSim. In this work it is a two-port component in CircSim. This component represents the original antenna.

4) Passive components of the feeding network are connected to the two-port component in CircSim. Generators and generator impedances are connected to the feeding network as well.

5) The Z-matrix and the embedded element patterns of the original antenna are loaded into MPA. MPA communicates with CircSim and asks CircSim to compute the currents in the antenna ports. These currents together with the Z-matrix and the embedded patterns of original antenna makes it possible for MPA to compute radiation parameters of the antenna with connected network.

6) MPA evaluates the results and changes component values which are sent back to CircSim which now can compute new currents.

7) Steps 5 and 6 are repeated in the optimization loop until a satisfactorily result has been achieved (or the maximum number of iterations is reached).

Having done these steps, one can start optimization. It is possible to select different goal functions in MPA. For instance it is possible to set the goal for highest value of diversity gain, efficiency, effective diversity gain or the lowest correlation value. It is also possible to use different weightings for different goals. In this work different settings were tried and as a conclusion the best choice to choose is to set optimization goal for highest efficiency and diversity gain, otherwise by just selecting efficiency it is possible that correlation increases and therefore effective diversity gain does not improve very much. Also another reason is that if only efficiency is selected as goal function, it is possible that MPA software optimizes merely for efficiency of one of the antenna elements and efficiency for the other element drops. Therefore, both efficiency and diversity gain was chosen for optimizations. It is also possible to choose one or more frequencies for optimizations.

Optimization has been done for network1 and network2 for discrete frequencies of 800/900/1800/2100/2700. The result of optimization shows that for network1 and network2 it is possible to achieve 9 to 9.5 dB effective diversity gain at each frequency of interest. But since optimization has been done per frequencies, Z1-Z3 reactance values varies with frequencies in a non-physical way. Therefore, it is not possible to realize them by a single inductor or capacitor for the whole frequency band. However, non-foster network, which might be possible to realize with active components, can make this wideband solution possible.

Figure 4.7 shows optimization results for effective diversity gain. One optimization is done for each single frequency. This means that for each frequency different inductance and capacitance values are needed. Reactance values for Z1-Z3 is shown in Figure 4.8 for different frequencies.

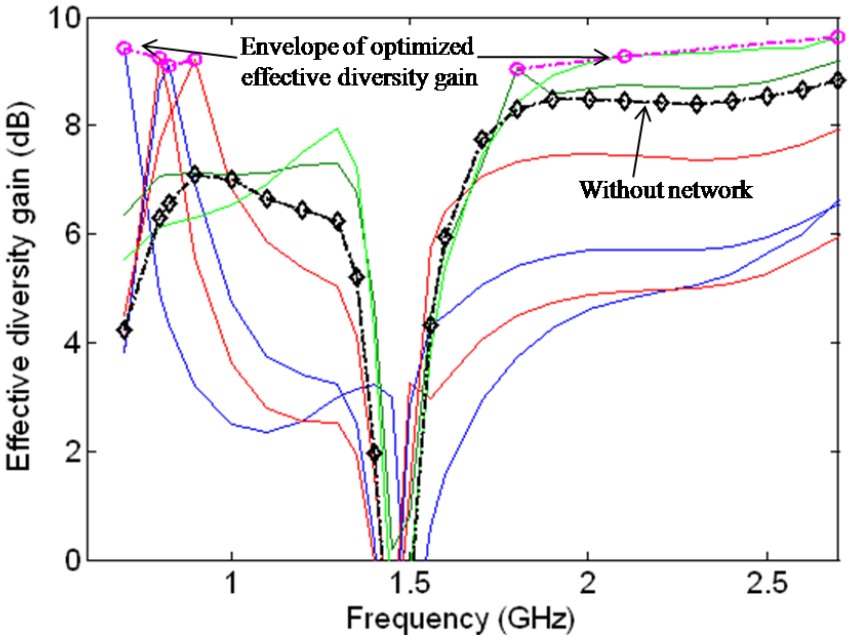

Figure 4.7 *Effective diversity gain, the results achieved by optimization for each frequency.*

Since the antenna structure is symmetric, Z1 should be equal to Z2. As can be seen in Figure 4.8, MPA also gave equal values for Z1 and Z2 as it should be expected. In Figure 4.8, slope of reactance curve for Z1 and Z2 in the lower frequencies and also slope of reactance curve for Z3 in all frequencies is negative. This means that negative inductors or capacitors –which do not exist in real world- are needed in order to make such a behavior. Such networks might be possible to realize with non-Foster network.

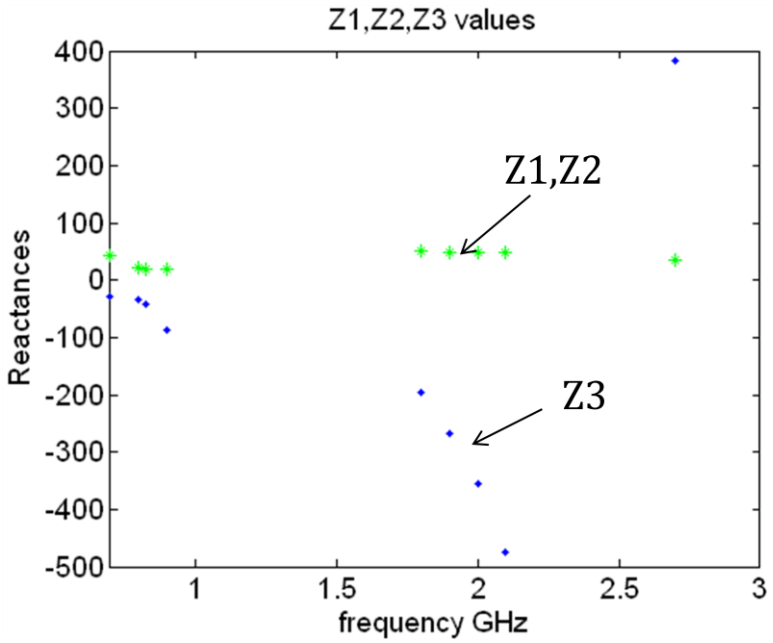

Figure 4.8 *Reactance values versus frequency.*

One guess is that it might be possible to replace each complex impedance with a network consisting of several inductors and capacitors so that a wider frequency band can be covered. To investigate this, an impedance estimator software (ImpEst [18]) was used to see if it is possible to realize each of the complex impedances with a number of inductors and/or capacitors. But no network was found for the complex reactances Z1, Z2 and Z3.

Next logical step that comes in mind is to test networks with more components to investigate if it can give a more wideband solution.

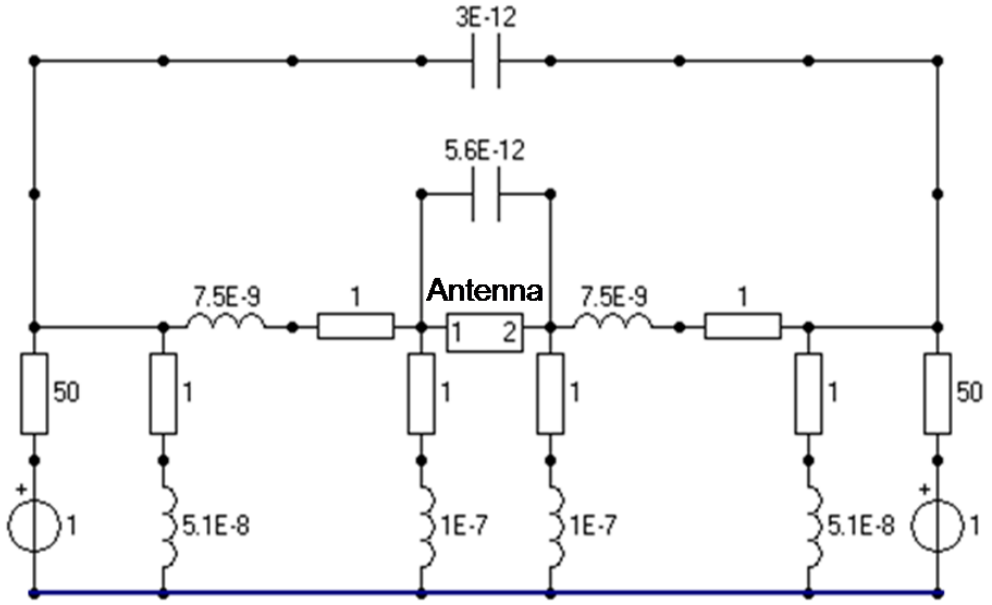

Figure 4.9 Network9 with passive components, optimization for 800-900 MHz.

Figure 4.9 shows a more complex network. Optimization has been done at 800 and 900 MHz for this network. Values of capacitors and inductors for network9 are shown in the Figure 4.9. One ohm resistors are connected in series with each inductor in order to model losses in real components.

Once optimization results looks acceptable then reactance values should be computed and converted to capacitor and inductor values. The last optimization should be done with having capacitors and inductors instead of reactances; also losses of components should be included in the last optimizations for accuracy of results.

Figure 4.10 and Figure *4.11* shows optimization results of S11 and S21 for antenna with network9 in comparison with the antenna without network. Improvement for reflection coefficient and mutual coupling are achieved at 0.8 and 0.9 GHz. S11 is below -6 dB from 700 to 966 MHz. S21 is below -10 dB in two frequency spans from 740 to 854 MHz and from 925 up to 1095 MHz.

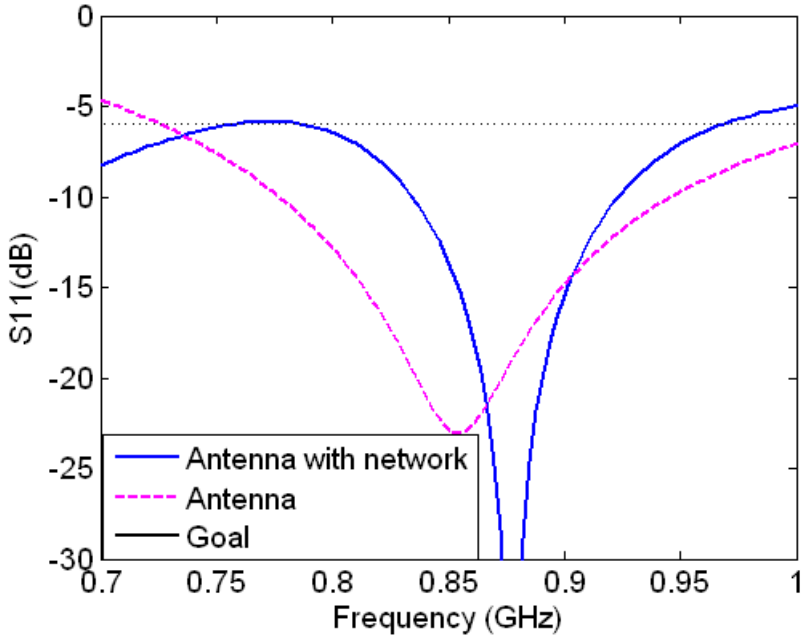

Figure 4.10 Simulated S11 for antenna and antenna with network9 from 0.7 to 1 GHz.

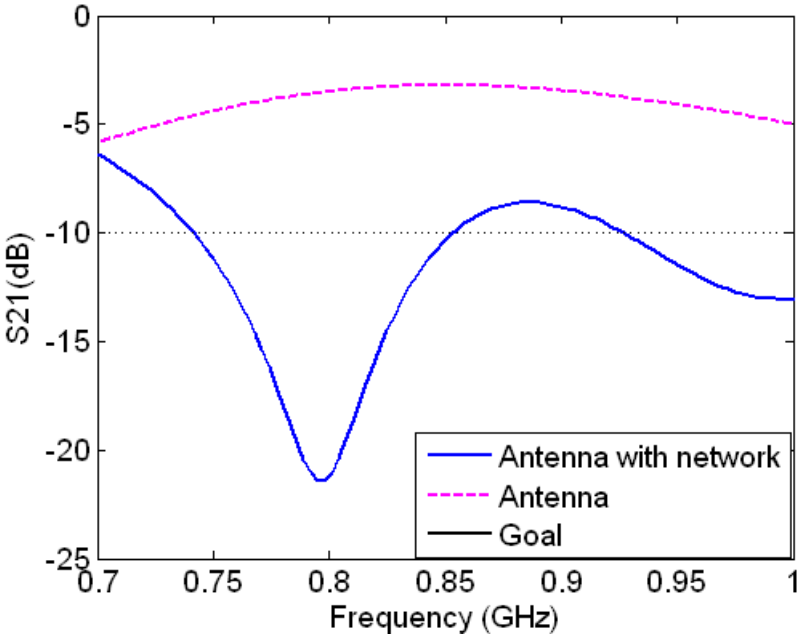

Figure 4.11 Simulated S11 for antenna and antenna with network9 from 0.7 to 1 GHz.

Figure 4.12 shows comparison between simulation results of effective diversity gain for antenna with and without passive network9. The optimization is done for 800-900 MHz frequency band. 825 MHz is also included in optimizations to be sure that efficiency does not drop between 800 and 900 MHz. Effective diversity gain improves to 8.6 dB at 800 MHz and 8.8 dB at 900 MHz.

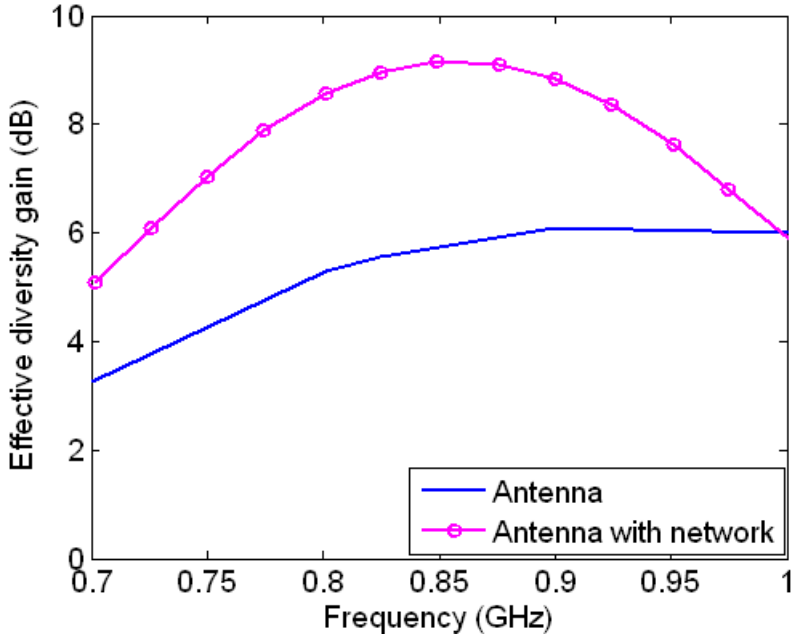

Figure 4.12 Effective diversity gain, original antenna and antenna with network.

It should be added that when optimization runs at one single frequency, it is possible to achieve high effective diversity gain of 9.8 dB but when the goal is set for more frequencies - 800, 825 and 900 in this optimization-, values for effective diversity gain drops 1 or 1.5 dB at each frequency. And even with this complex topology, MPA does not find improved performance at all frequencies of interest. In other words, the cost of low frequency improvement is degradation of high frequency performance.

Figure 4.13 shows a complex network topology. Optimization has been done at 1800, 2100 and 2700 MHz. Reactance values are computed and converted to capacitor and inductor values which are shown in the figure. Also one ohm resistor is considered for each inductor due to existing losses in real components.

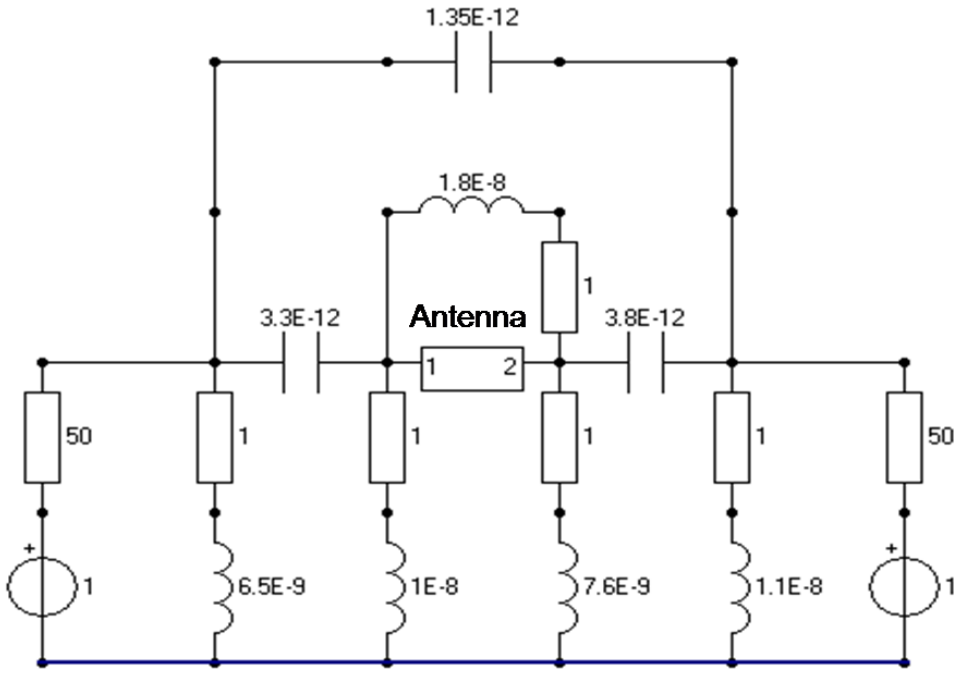

Figure 4.13 Network10 with passive components, optimization has been done for 1800-2100-2700 MHz.

Figure 4.14 and Figure 4.15 shows optimization results of S11 and S21 for antenna with network10 in comparison with the antenna without network. Improvement for reflection coefficient obtained for the whole frequency band from 1.8 to 2.7 GHz. Mutual coupling is below -10 dB from 1.8 to 2.51 GHz, but at 2.7 GHz, it is -8.65 dB.

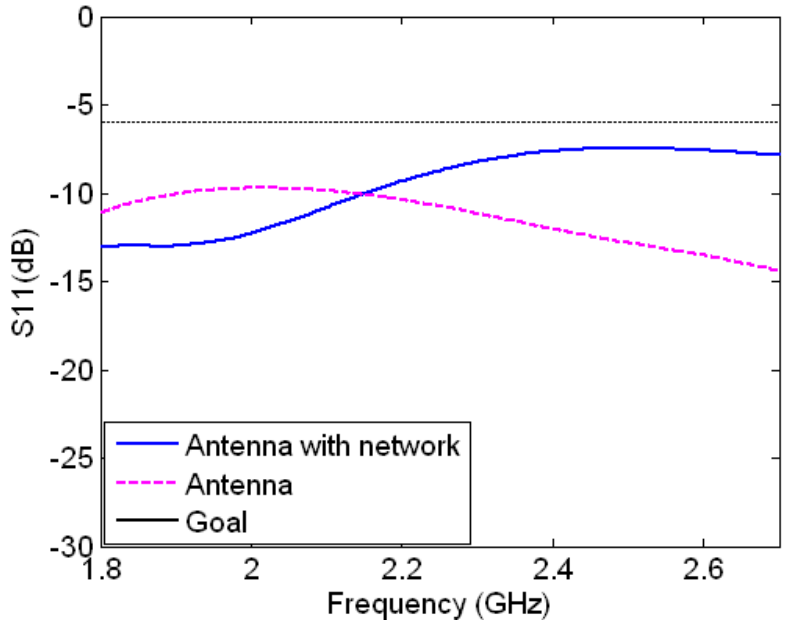

Figure 4.14 Simulated S11 for antenna and antenna with network10 from 1.8 to 2.7 GHz.

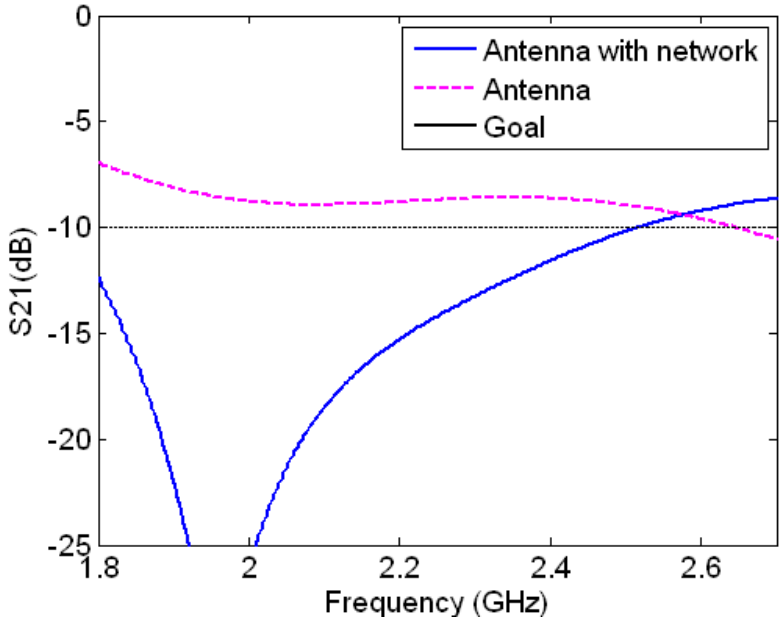

Figure 4.15 Simulated S21 for antenna and antenna with network10 from 1.8 to 2.7 GHz.

Figure 4.16 shows comparison between simulation results for effective diversity gain of antenna with and without passive network10. The optimization is done for 1800-2100-2700 MHz frequencies. Effective diversity gain reaches to 9.4 dB at both 1.8 GHz and 2.1 GHz but at 2.7 GHz it drops to 7.5 dB. Also with network10 high frequency performance improves where low frequency performance becomes worse.

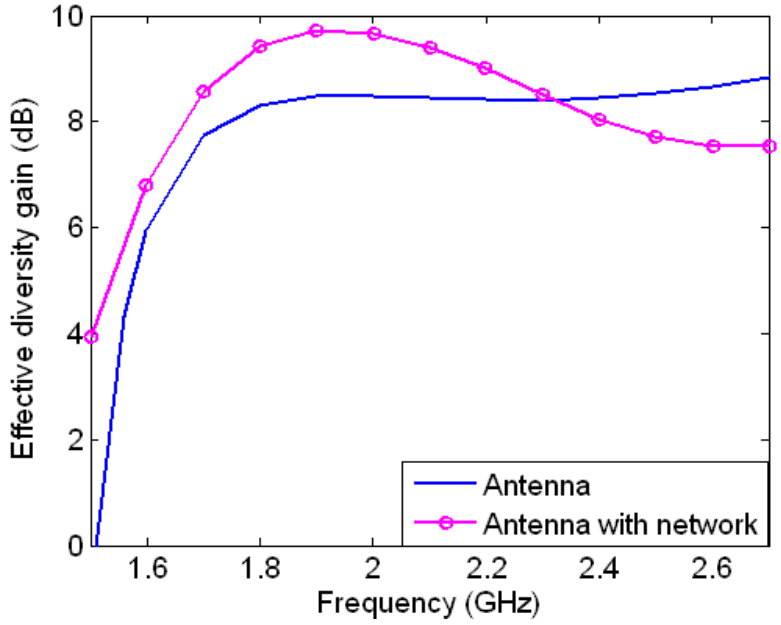

Figure 4.16 Effective diversity gain, original antenna and Antenna with network.

According to optimization results, with the two founded network9 and network10, it is possible to improve antenna performance at wanted frequencies of interest 800/900/1800/2100 MHz.

5 Final Realization of Antenna Including Matching Network

Having done the optimization, it comes the right time for manufacturing the antenna with the feeding network connected to it. Figure 5.1 shows the scheme of antenna with connected feeding network. Capacitors and inductors are shown as green boxes and transmission lines between components are shown as black lines. Grounds and two ports are shown in the figure as well.

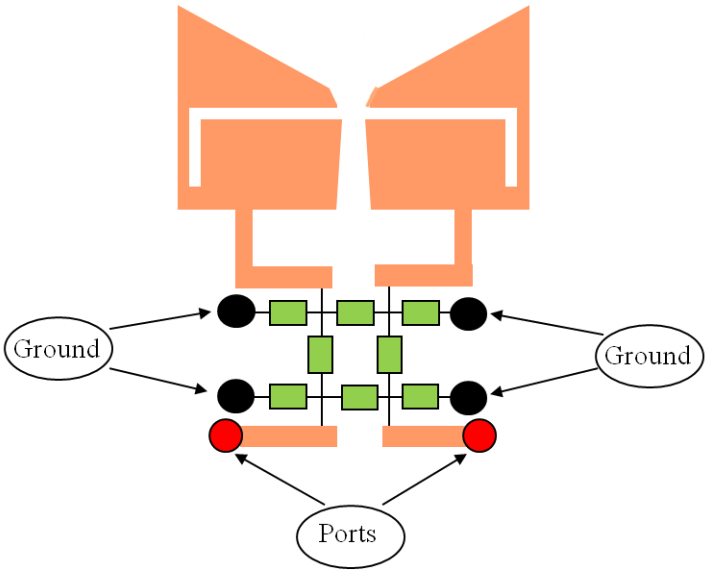

Figure 5.1 Antenna with connected feeding network scheme.

However, when comes to realization, it is needed to design the feeding pad where capacitors and inductors are going to be mounted. Designing of pads is done in CST. In order to reduce the effect of coupling between microstrip lines placed between components, feeding pads should be as small as possible and close to the antenna ports similar to how the network looks like in Figure 5.1.

In Figure 5.2, antenna is shown with the designed feeding network which is done in CST. Transmission lines of feeding network are placed as close as possible to the antenna elements. Also inductors and capacitors are placed as close as possible in the network, in order to reduce the effect of parasitic capacitances due to the close by transmission lines.

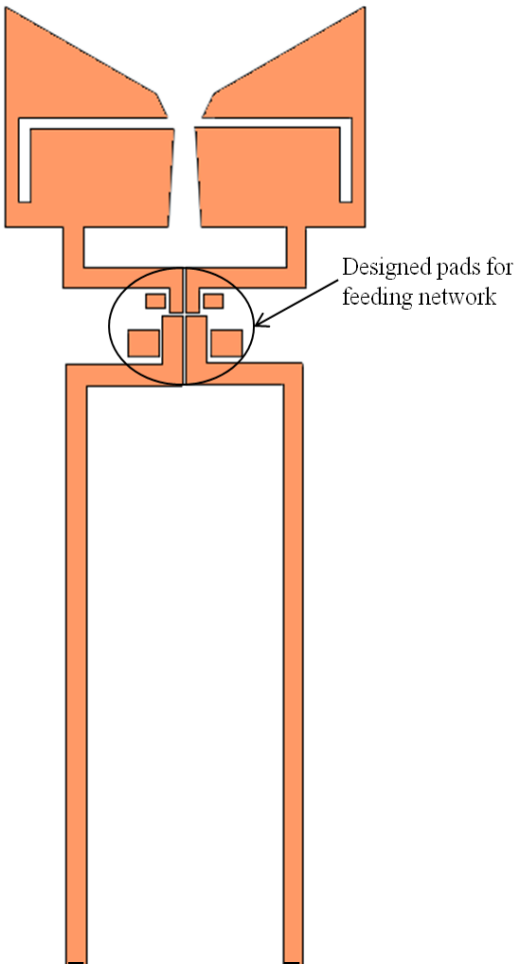

Figure 5.2 Designed pads for feeding network.

Next step is to manufacture the antenna including feeding pads and to mount the components on the antenna PCB. The antenna is manufactured with etching method at SP.

Figure 5.3 Manufacturing the antenna at SP.

Components are ordered from Murata manufacturing company. Inductors are LQG18H series 0603 size. These inductors are designed to realize stable characteristics for high frequencies by using a multilayer process. They are suitable for high frequency circuits of mobile communication equipments. Capacitors are ceramic monolithic size 0603 from Murata manufacturing company for high frequency applications. Size of components is 1.6 x 0.8 mm which is very small to handle for soldering [18].

In the left part of Figure 5.4 Prototype of antenna with matching network (left), Zoomed view of realized network with lumped components., the manufactured antenna with feeding network is shown and in the right part of the figure a close up view of the feeding network with mounted capacitors and inductors is shown. Capacitors are in gray color and inductors are in blue color.

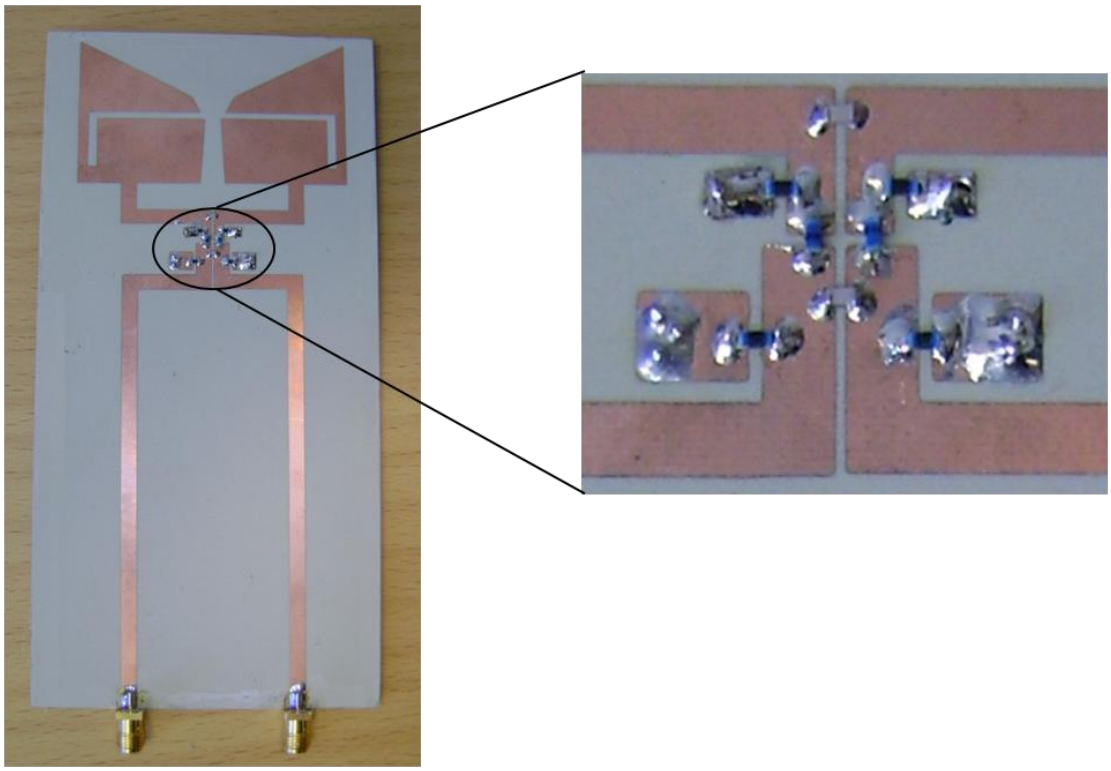

Figure 5.4 Prototype of antenna with matching network (left), Zoomed view of realized network with lumped components.

In the next chapter, you will see the results from measurement of the manufactured antenna in comparison with simulation results.

5.1 Measurement and Simulated Results

Measurement has been done in Reverberation chamber at Chalmers antenna lab. In this part, you will see the figures including measurements of antenna with and without network and simulations results of the antenna with and without network to compare with. Feeding network were designed and optimized by MPA to improve radiation performance of the antenna at 800 and 900 MHz. Simulation of the antenna without network has been done by CST MS.

Simulation and measurement of S11 and S21 for original antenna and antenna with network are shown in Figure 5.5 and Figure 5.6 respectively. As can be seen in Figure 5.5, there is a frequency shift of 20 MHz between simulation and measurement result of S11 for original antenna. For antenna with network, S11 is below -10 dB in the whole frequency band of 700-900 MHz.

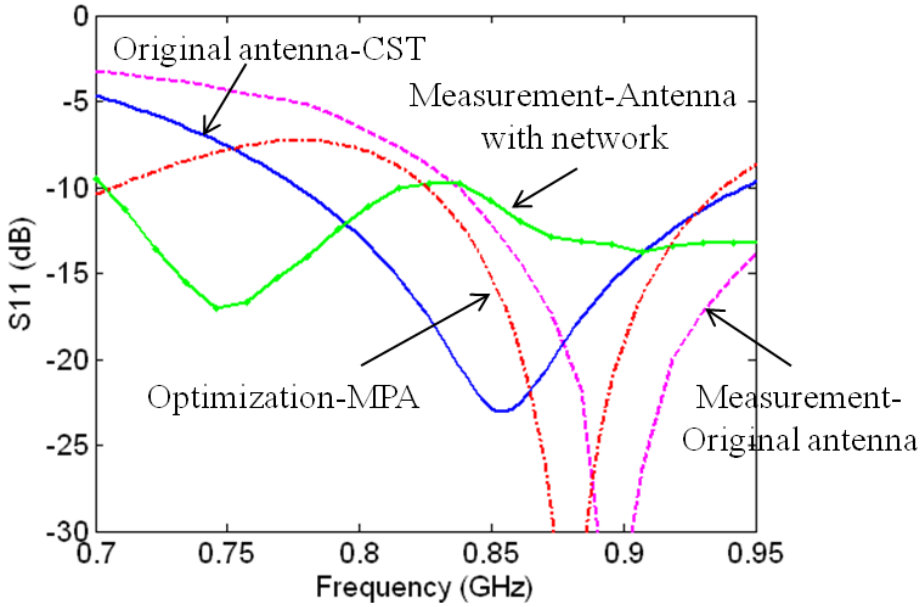

Figure 5.5 *Measured and simulated of S11 for original antenna and antenna with network9.*

As can be seen in Figure 5.6, measured S21 of the original antenna is in good agreement with simulation. But measured mutual coupling for antenna with network is higher than the given simulated data by MPA. A shift in the frequency of measured data in comparison with MPA simulation can be seen in the figure as well.

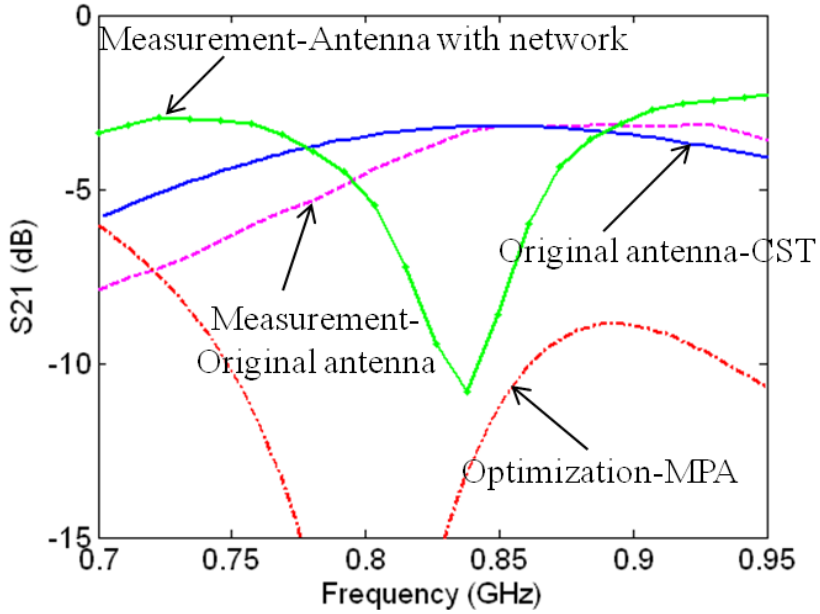

Figure 5.6 *Measurement and simulation of S21 for original antenna and antenna with network9.*

Figure 5.7 shows the simulations and measurements for correlation coefficient of original antenna and antenna with network9. Measured envelope correlation coefficient for antenna with network is below 0.2 from 730 to 870 MHz and is below 0.4 from 700 up to 886 MHz as is shown in the figure below.

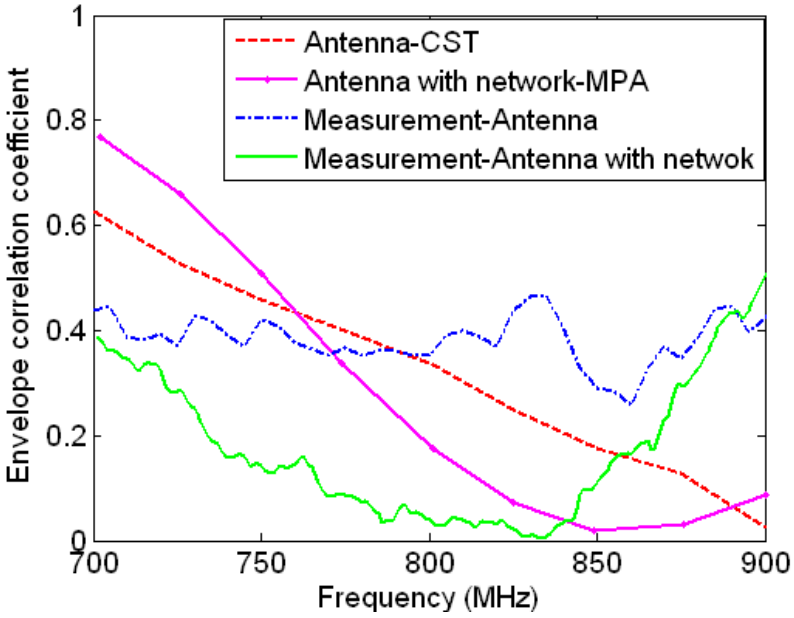

Figure 5.7 *Measurements and simulations for envelope correlation coefficient for original antenna and antenna with network9.*

Measurements and simulations for efficiency of original and antenna with network are shown in Figure 5.8. Measured Efficiency of antenna with network is -2 dB with 2.5 dB improvement in 804 MHz in comparison with measured efficiency of original antenna. But at 900MHz it decreases 2.5 dB which is not in agreement with MPA optimization results. Possible reasons will be explained in the next chapter.

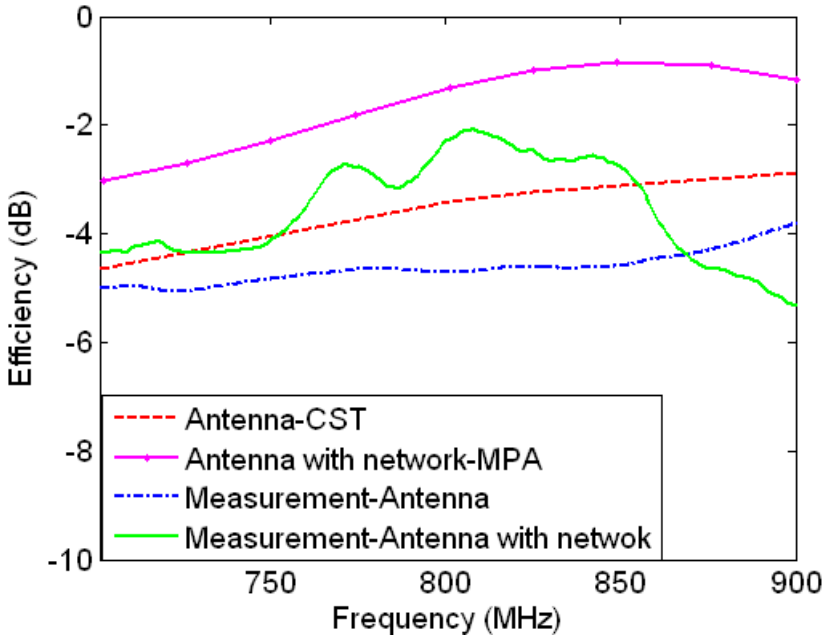

Figure 5.8 *Measurements and simulations for efficiency of original antenna and antenna with network9.*

Figure 5.9 shows simulations and measurements for apparent diversity gain of original antenna and antenna with network9. Measurement data for apparent diversity gain of original antenna is in a good agreement with simulation at frequency of 800 to 1000 MHz. Measured value for apparent diversity gain of antenna with network9 is 10.14 dB at 800 MHz and 8.7 dB at 900 MHz .

However, there is a shift in the frequency between measured data of apparent diversity gain of antenna with network and simulation from MPA.

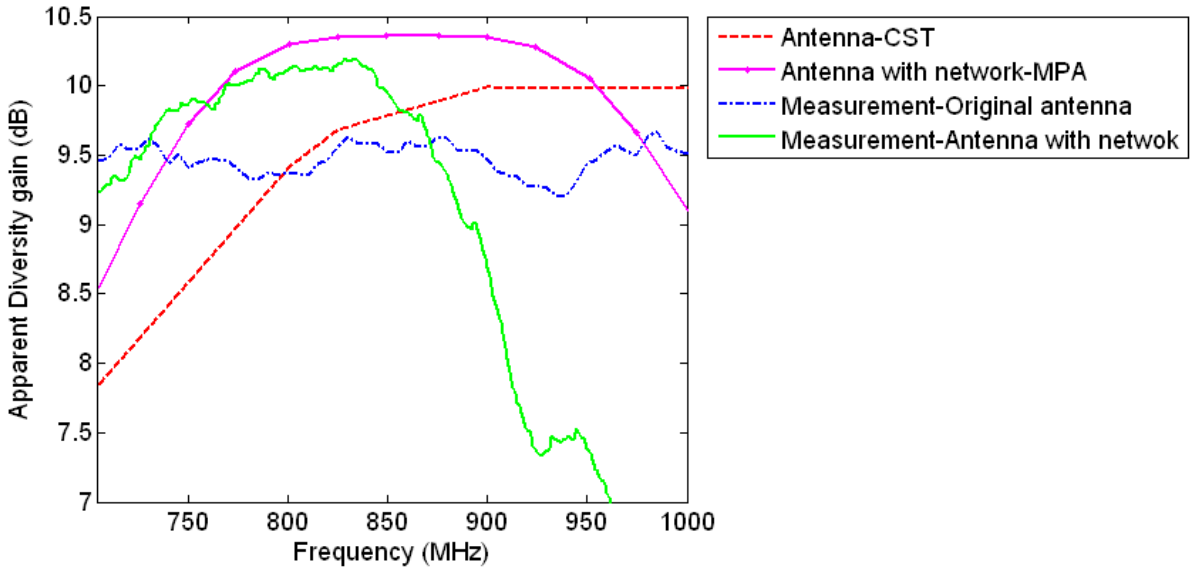

Figure 5.9 *Measurements and simulations for apparent diversity gain of original antenna and antenna with network9.*

Figure 5.10 shows simulations and measurements for effective diversity gain of original antenna and antenna with network9. Measured value for effective diversity gain of antenna with network9 is 8 dB at 800 MHz with 2.5 dB improvement compare to the original antenna, but it drops to 3.5 dB at 900 MHz which is a 5.2 dB difference compared with MPA simulation at 900 MHz .

There is a shift in the frequency between measured data of effective diversity gain of antenna with network and simulation from MPA as well.

In the next part, I will explain the possible reasons behind the difference in measurement and simulations and also the frequency shift between them.

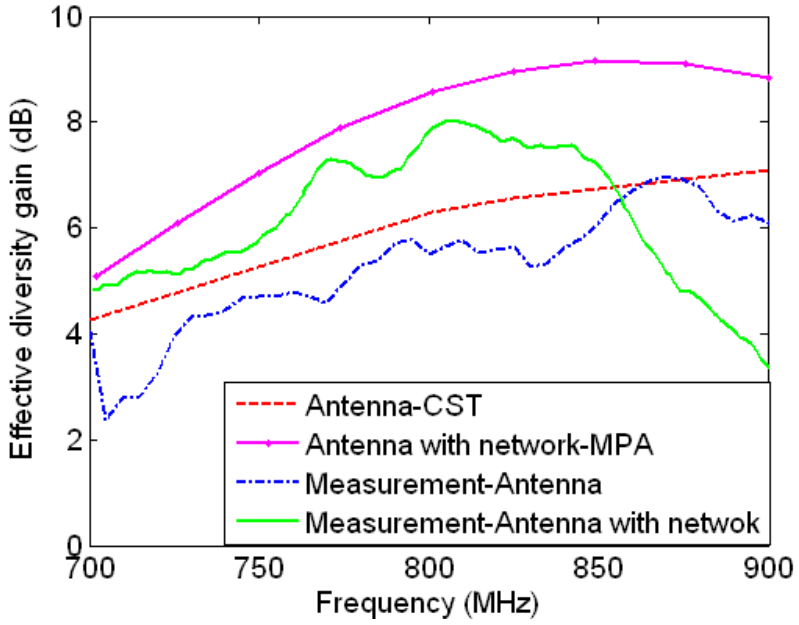

Figure 5.10 *Measurements and simulations for effective diversity gain of original antenna and antenna with network9.*

5.2 Reasons for difference between measurements and MPA

There is not a good agreement between measurement results and simulations in MPA of antenna with network, especially at 900 MHz. Also measured effective diversity gain is lower than what is expected from MPA simulation. One possible reason could be that losses in the passive components is different and higher than what is expected from datasheet. And also it changes with frequency.
To figure out this fact, I include 10 ohm resistors to model loss for each of the inductors and compute the effective diversity gain.

Figure 5.11 shows the simulation result for effective diversity gain of antenna with connected components with ten ohm loss in comparison with measurement of antenna with network9 and simulation with components with one ohm loss by MPA.

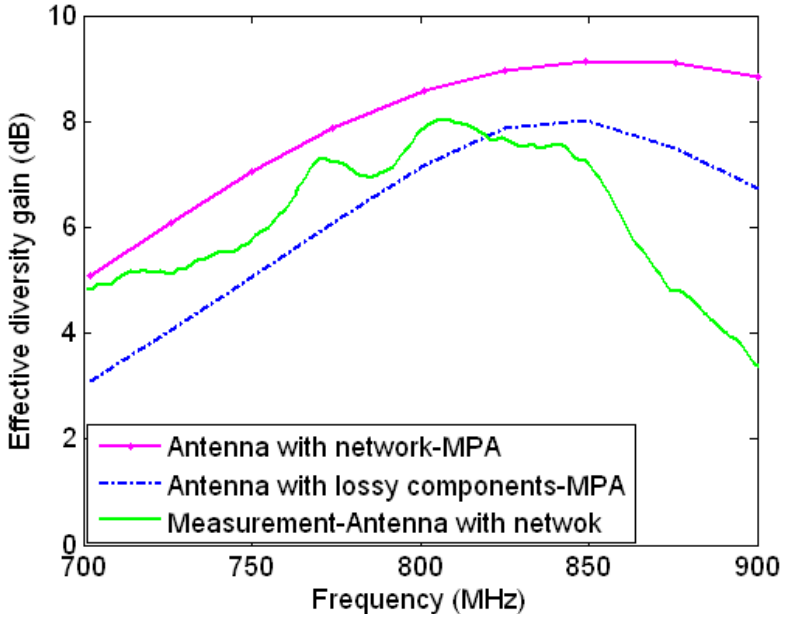

Figure 5.11 Measurements and simulations for effective diversity gain of antenna with lossy network and antenna with network9.

As can be seen in Figure 5.11, there is a better agreement between measurement and simulation of antenna with connected components with 10 ohm losses. By including 10 ohm losses in inductances, effective diversity gain decreases by 2dB.

Still there is a disagreement, so in order to explain this, the antenna is modelled in CST including passive components and transmission lines to the ports.

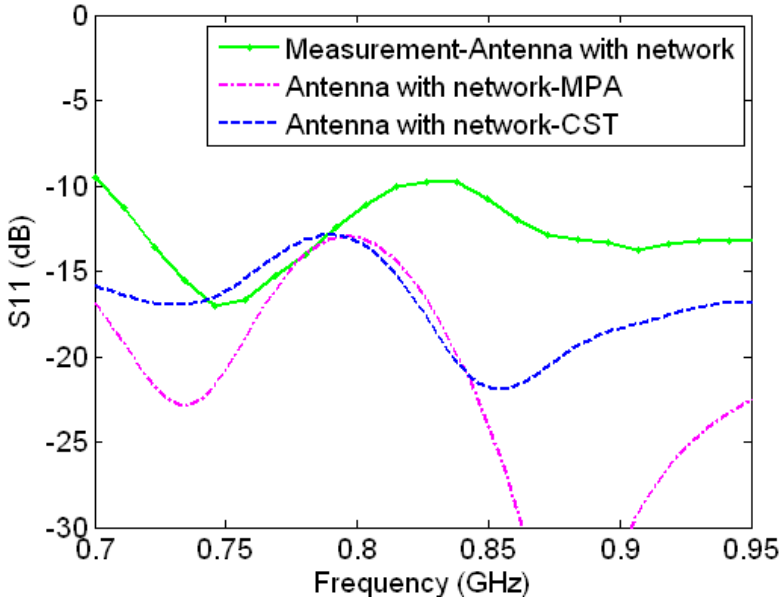

Figure 5.12 Measured S11 and simulated S11 by MPA and CST.

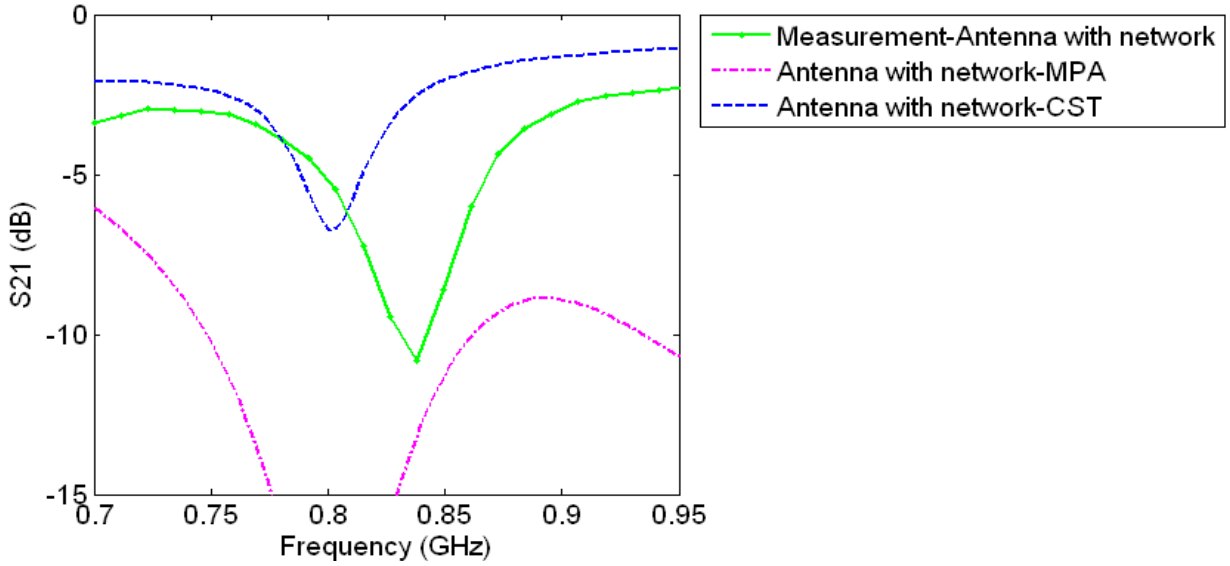

Figure 5.13 Measured S21 and simulated S21 by MPA and CST.

As can be seen in Figure 5.12 and Figure 5.13, there is a better agreement between measured and simulated S11 and S21 of the antenna with network and transmission lines to the ports by CST. It means that transmission lines will also affect the S-parameters. However, there is still a frequency shift for measured effective diversity gain, this can be due to the fact that lumped circuit components are not ideal. In the CST simulation the lumped components are ideal whereas, the capacitances and inductances are not ideal in measurement. The soldering iron that is used for mounting components also makes some changes in the value of capacitances and inductances.

An improvement of the work presented in this thesis would be to simulate the transmission lines between the ports at the feeding network and the ports at the end of the PCB (i.e. at the SMA-connectors) as a four-port component in CST, see Fig. 5.14. Then, the computed S-

matrix could be imported in CircSim as a component. By doing this the effect of transmission lines could be taken into account and the agreement between measurements and simulations in MPA would probably be better.

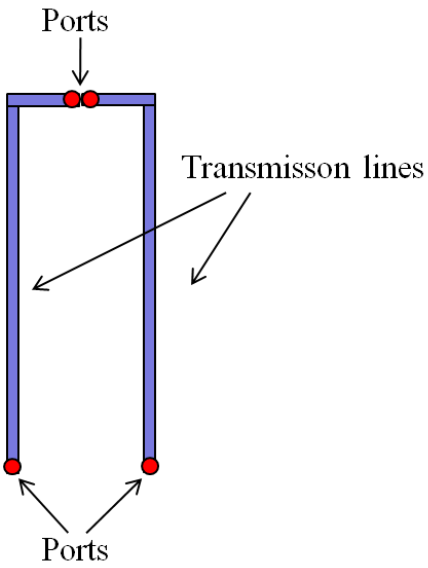

Figure 5.14 Transmission lines as a four-port component.

In should be mention that, it is not possible to include the added transmission lines -where lumped components are mounted on- in the simulation of the original antenna. And having this transmission lines in vicinity of components will also change the values of passive components. Hence this is another reason for disagreement between measurements and simulations.

6 Conclusion and Suggestion of Future Work

This report includes the explanation of the method of designing a passive network to improve the radiation performance of a multi-port antenna with MPA software. CST MS software has been used as a full wave simulator tool to simulate the original antenna. MPA together with CircSim is used for optimization and computation of radiation properties of the antenna. There are several steps that are needed to be done to make CircSim and MPA work together. This is in principle time consuming especially if number of antenna elements increases or number of frequency points needed for optimization increases. Then the designer needs to export all the data for radiation pattern of each antenna element at every frequency of interest. Also for a good resolution in computed data, it is needed to export the radiation pattern of each antenna element at more frequency points in addition to the frequencies of interest. Also CircSim needs Z matrix, thus it is needed to convert S matrix to Z matrix and then import it to CircSim. It is of importance to import the Z matrix to MPA only for the frequencies of interest; this means that the number of frequency points in radiation pattern and Z matrix should be equal and in order to do that one needs to interpolate the Z matrix. However the procedures for using MPA and CircSim is easy to understand and also the interfaces of MPA and CircSim are quite simple and easy to work with.

As a result of this work, networks have been designed for a given two-port antenna to improve performance. With a simple topology consisting of three passive components, as described in 4.1, it is possible to achieve improvement in effective diversity gain at each frequency of interest. However, wide-band/Multi-band design is challenging. Two network topologies are designed to improve radiation performance at multi-bands of 800/900/1800/2100/2700. Network9 is designed for improvement between 800 and 900 MHz and network10 is designed for improvement at 1800/2100/2700. Also the original antenna is scaled and modified for better performance at lower frequency band of 700 MHz to 3 GHz. To validate the design in MPA, the antenna, including the passive network, was manufactured and then measured. Improvement in effective diversity gain is achieved from 700 to 860 MHz. Measured value for effective diversity gain of antenna with network9 is 8 dB at 800 MHz but it drops to 3.5 dB at 900 MHz which differs 5.2 dB compared with MPA simulation at 900 MHz. To figure out the reason for the difference between simulation by MPA and measurement, another simulation is done including lossy components, modeled with 10 ohm resistors for each inductor. The agreement between simulation and measurement becomes better when losses are included and simulation results shows that diversity gain drops 2 dB because of components with 10 ohm loss. Even better agreement has been obtained between measured and simulated S11 and S21 when the antenna is simulated in CST including components and transmission lines to the ports. To obtain better simulation results from MPA, it is possible to introduce transmission lines to the ports. This can be done by computing the four-port S-matrix for the transmission lines in CST and import it as a component in CircSim. It is suggested that this is done as a continuation of this work.

Another suggestion for future work for similar projects could be to design an active feeding network or to use a varactor which has tunable reactance or a component with negative slope of reactance versus frequency to see if it is possible to achieve a multi-band solution merely with one network.

7 References

[1] Computer code CST MWS, http://www.cst.de

[2] Kristian Karlsson, Jan Carlsson, Ilja Belov, Per-Simon Kildal, "Software for Optimizing Multi-port Antennas Based on Precomputed Embedded Element Patterns from Commercial Codes", 2007, EMB07 Computational Electromagnetics - Methods and Applications, October 18-19 2007, Lund, Sweden.

[3] P-S Kildal, *Foundations of Antennas*, Compendium in Antenna Engineering at Chalmers, Spring 2009.

[4] K. Karlsson, Embedded Element Patterns in Combination with Circuit Simulations for Multi-Port Antenna Analysis, PhD thesis, Chalmers University of Technology, Sweden, Oct. 2, 2009.

[5] D.F. Kelley, ''Embedded element patterns and mutual impedance matrices in the terminated phased array environment'', Proceedings of IEEE AP-S International Symposium, vol. 3A, pp. 659-662, USA, 3-8 July 2005.

[6] N. Pierce and S. Stein, "Multiple diversity with nonindependent fading", Proceedings of the IRE, pp. 89-104, 1960.

[7] M. V. Ivashina, M. Ng Mou Kehn, P.-S. Kildal and R. Maaskant, "Decoupling efficiency of a wideband Vivaldi focal plane array feeding a reflector antenna", IEEE Transactions on Antennas and Propagation, Vol. 57, N0. 2, pp 373-382, Feb. 2009.

[8] M. Ng Mou Kehn, M. V. Ivashina, P.-S. Kildal and R. Maaskant, "Definition of unifying decoupling efficiency of different array antennas - case study of dense focal plane array feed for parabolic reflector", AEUE-International Journal of Electronics and Communications, 2009 - Elsevier, available on line 4 June 2009.

[9] Per-Simon Kildal, Kent Rosengren, "Electromagnetic Analysis of Effective and Apparent Diversity Gain of Two Parallel Dipoles", IEEE Antennas and Wireless Propagation Letters. Vol.2, 2003.

[10] A. Hussain, P-S. Kildal, U. Carlberg, J. Carlsson "Analysis of Statistical Uncertainties Involved in Estimating Ergodic MIMO Capacity and Diversity Gain in Rayleigh Faded Environment" accepted for publication in ICECom 2010, Dubrovnik, Croatia.

[11] N. Jamaly, P-S Kildal and J. Carlsson, ''Compact formulas for diversity gain of two port antennas'', 'To be published in IEEE Antennas and Wireless Propagation Letters'.

[12] Anders Derneryd, Jonas Fridén, Patrik Persson, Anders Stjernman , '' Performance of closely Spaced Multiple Antennas for Terminal Applications'', Antennas and propagation, EuCAP 2009, pp 1612 – 1616, March 2009.

[13] Kristian Karlsson, Jan Carlsson, ''Circuit Based Optimization of Radiation Charactristics of Single and Multi-Port Antennas'', SP Technical Research of Sweden.

[14] S. Zhang, Z. Ying, J. Xiong, S. He, ''Ultra wideband MIMO/Diversity Antennas with a Tree-like Structure to Enhance Wideband Isolation'', IEEE Antennas and Wireless Propagation Letters, Vol.8, 2009.

[15] K.L Wong, S. W. Su, and Y. L. Kuo, "A printed ultra-wideband diversity monopole antenna," Microw. Opt. Technol. Lett., vol. 38, no. 4, pp. 257–259, 2003.

[16] T.S.P. See and Z. N. Chen, "An ultrawideband diversity antenna," IEEE Trans. Antennas Propag., vol. 57, no. 6, pp. 1597–1605, Jun. 2009.

[17] CircSim, Circuit simulator program based on MNA, J. Carlsson, http://www.sp.se, jan.carlsson@sp.se

[18] ImpEst, Impedance estimator program developed in Chase MIMO Terminals, K. Karlsson.

[19] Murata, Datasheet, http://www.murata.com/products/catalog/pdf/o05e.pdf#LQG18H